 doi:10.20944/preprints202206.0214.v1

*Article*

# Theory and Applications of the (Cardio) Genomic Fabric Approach to Post-Ischemic and Hypoxia-Induced Heart Failure

**Dumitru Andrei Iacobas** [1,*] **and Lei Xi** [2,*]

[1] Personalized Genomics Laboratory, CRI Center for Computational Systems Biology, Roy G Perry College of Engineering, Prairie View A&M University, Prairie View, TX 77446, U.S.A.; E-mail: daiacobas@pvamu.edu
[2] Pauley Heart Center, Division of Cardiology, Virginia Commonwealth University, Richmond, VA 23298, U.S.A. E-mail: lei.xi@vcuhealth.org
* Correspondence: daiacobas@pvamu.edu (DAI), lei.xi@vcuhealth.org (LX)

**Abstract:** Decades of research identified numerous gene biomarkers of cardiac diseases whose restored sequence or/and expression level was hoped to recover the normal cardiac function. However, each human has unique and dynamic pathophysiological characteristics resulting from the unrepeatable combination of favoring factors such are: race, sex, age, medical history, diet, stress, exposure to toxins, habits etc. As such, no treatment fits everybody and finding personalized solutions is a top priority for medicine of 21st century. The Genomic Fabric Paradigm (GFP) provides the most theoretically possible comprehensive characterization of the transcriptome, its alterations in disease and recovery following a treatment. By attaching to each gene the independent average expression level, expression variation and expression coordination with each other gene, GFP delivers thousands times more information than the traditional analysis. This report presents the theoretical bases of the GFP and some applications to our microarray data from mouse models of post ischemic, and constant and intermittent hypoxia-induced heart failure. The GFP analyses revealed novel transcriptomic aspects of the gene expression control and networking under ischemic conditions. Through all-inclusive characterization of the transcriptome and the unrepeatable gene hierarchy in each condition, GFP is an essential avenue towards development of a truly personalized cardiogenomic therapy.

**Keywords:** Adra1b; cardiac ischemia; hypoxia; Crem; gene expression control; gene expression coordination; gene hierarchy; heart failure; transcriptomic stoichiometry

## 1. Introduction

Personalized or precision medicine has become a focal area of interests and development in medicine of 21st century. This is because the individual variances of biological response to environmental factors and drug therapies may substantially alter the outcomes of disease progression and therapeutic success. Understanding the genomic and epigenetic mechanisms regulating these variabilities due to the factors, such as race, sex, age, medical history, diet, stress, exposure to toxins, and individual habits, etc., could be critical for designing clinical strategy tailored for each patient. For example, 70 microRNAs identified in whole blood samples via next generation sequencing were linked to the risk of recurrent myocardial infarction and future stent thrombosis, as compared to coronary artery disease (CAD) patients without the subsequent events [1]. The miRNA profiling may be used to identify individuals at high risk for proper treatment or intervention. A recent review elegantly summarized advances that unravel the genetic architecture of CAD with approximately 60 genetic loci to CAD risk [2]. These authors suggested that genetic testing could enable precision medicine approaches by identifying subgroups of patients at increased risk of CAD or with a specific driving pathophysiology that can be targeted precisely [2].

 doi:10.20944/preprints202206.0214.v1

A very rich literature brings rationale and experimental evidence for several molecular mechanisms that might be responsible for a spectrum of cardiomyopathies. Gene expression profiling is now considered a very important tool to individualize the pathophysiological characteristics and tailor the appropriate therapy for each individual (e.g.: [3-5]) but do we utilize the expression data at their full potential? As we will prove in this report, traditional quantification of the transcriptomic alteration, limited to determining the percentages of up/down-regulated and turned on/off genes, neglects over 99% of the information provided by any high-throughput gene expression platforms. Therefore, we use the revolutionary Genomic Fabric Paradigm (GFP) [6] that, in addition to the average expression level (AVE) across biological replicas, characterizes each individual gene by the relative expression variability (REV) and the expression correlation (COR) with each-other gene.

REV is an indirect measure of the strength of the homeostatic mechanisms that keep the random fluctuations of the gene expression within a narrow interval. COR, accounting for the "Principle of Transcriptomic Stoichiometry" (PTS) [7], determines whether and how strongly the genes are networked in functional pathways. PTS, a generalization of Dalton's laws from chemistry, requires the coordinated expression of genes whose encoded products are participating to a functional pathway. GFP considers the transcriptome as a multi-dimensional mathematical object subjected to dynamic sets of homeostatic controlling mechanisms and expression correlations of the individual genes. Thus, GFP gives the most theoretically possible comprehensive characterization of the transcriptome topology, increasing the workable information by 4 orders of magnitude.

In previous publications, we have shown that the transcriptome topology is strongly dependent on race/strain [8], sex [9], age [10] and region of the profiled tissue [6]. In addition to these general factors, the transcriptome topology is also very sensitive to the individual's own characteristics like: medical history [11], diet [12], treatment [13], local stimuli [14] and a wide diversity of habits and exposure to stress [15] and infections [16, 17]. As subjected to unrepeatable combinations of influential factors, some of them changing in time, each human is a dynamic unique and therefore the medial treatment should be tailored to the today's characteristics of the patient. This report presents the theoretical bases of the (cardio) genomic fabric approach, an important step towards development of the personalized cardiology.

## 2. Materials and Methods

### *2.1. Experimental data*

The (cardio)genomic fabric approach is illustrated here by using publicly available microarray data from a mouse model of post-ischemic heart failure (PIHF) [18, 19] and from mice subjected to chronic constant (CCH) or intermittent (CIH) hypoxia during their first 1, 2 or 4 weeks of life [20]. In all these experiments, the gene expression was profiled in the left ventricle of each of the four mice in every experimental group using 32k mouse oligonucleotide microarrays printed by the Albert Einstein College of Medicine, Bronx, NY, U.S.A.

As described previously in [11], 8 – 10 weeks old (20.5 – 25.5 g) male and female C57BL/6 mice, anesthetized with intraperitoneal injection of ketamine (40 mg/kg) and xylazine (80 mg/kg), were forced into myocardial infarction by permanently ligating the descending branch of the left coronary artery. Following development into PIHF, the mice were then injected into 3 regions at the borders of the cardiac scar with 10 µl Matrigel (BD Biosciences) with or without $1.5x10^6$ bone marrow mononuclear stem cells. Cells were suspended in Dulbecco's modified Eagle's medium (DMEM; Gibco, Grand Island, New York, USA) supplemented with 10% Fetal Bovine Serum, 100 U/ml penicillin and 100 mg/ml streptomycin [11]. The transcriptomes were profiled 59 days after induction of myocardial infarction induction and 49 days after cell therapy of the infarcted hearts. Total 12 mice (n = 4 per group) were used in this experiment and divided into: normal untreated ("NN"), infarcted untreated ("IN") and infarcted treated ("IT").

Preprints (www.preprints.org) | NOT PEER-REVIEWED | Posted: 15 June 2022 doi:10.20944/preprints202206.0214.v1

In the hypoxia study, neonatal CD1 mice were placed with their mothers in Biospherix hypoxia chambers in the second day of their life and kept there for the entire postnatal period of 1, 2 or 4 weeks. Three groups of 4 mice each, denoted by "N1", "N2", "N4", were kept under normal atmospheric conditions ($F_iO_2$ = 21%). For three groups of 4 mice each under chronic intermittent hypoxia (CIH), denoted by "I1", "I2", "I4", the fraction of inspired oxygen, $F_iO_2$ was alternated between 21% for 4 min and 11% for another 4 min, 24h/day. Finally, for other three groups of 4 mice each under chronic constant hypoxia (CCH), denoted by "C1", "C2", "C4", $F_iO_2$ was kept constant at 11% for the entire period [13]. CIH experiment was intended to model the episodic oxygen deprivation occurred in sleep apnea, while CCH experiment modeled the living at high altitude.

Although the datasets from both experiments were presented in previous publications [11, 13, 15, 21-23], the (cardio) genomic fabric approach was never used at its full potential and is able to reveal substantial novel and unpublished features for which the traditional analysis was incapable to delineate.

*2.2. Filtration and normalization*

All non-control spots with corrupted or saturated pixels, or with the median background fluorescence more than half of the median foreground signal in one array were eliminated from the analysis. The background subtracted foreground signal of each valid spot in one condition was normalized to the median of the background subtracted foreground signals of all valid spots in that condition.

*2.3. Characteristics of the (cardio) genomic fabric*

We define the (cardio) genomic fabric of a functional pathway in a particular region of myocardium as the transcriptome associated to the most interconnected and stably expressed gene network responsible for that pathway in that heart region.

Because the Agilent microarrays were printed with non-uniform numbers of spots probing redundantly the same gene, the independent characteristics AVE, REV, COR of individual genes probed by valid spots in each above defined condition were computing using the relations:

$$AVE_i^{(condition)} = \frac{1}{R_i}\sum_{k=1}^{R_i}\mu_{i,k}^{(condition)} = \frac{1}{R_i}\sum_{k=1}^{R_i}\left(\frac{1}{4}\sum_{j=1}^{4}a_{i,k,j}^{(condition)}\right) \quad , \quad where:$$

$$condition = "NN","IN","NT","IT","N1","N2","N4","I1","I2","I4","C1","C2","C4"$$

$R_i$ = number of spots probing redundantly gene "i", (1)

$a_{i,k,j}^{(condition)}$ = normalized expression level of gene "*i*" probed by spot "*k*" on biological replica "*j*" in "condition"

Our normalization procedure returns the AVE values in terms of the median gene expression level in that condition. For instance, AVE = 4.31 for prolactin receptor, (*Prlr*) in N1 means that the average expression of this gene is 4.31x larger than that of the median gene in N1 (like *Slc44a2* - Solute carrier family 44, member 2 whose AVE = 1.0005).

$$REV_i^{(condition)} = \underbrace{\frac{1}{2}\left(\sqrt{\frac{r_i}{\chi^2(r_i;0.975)}}+\sqrt{\frac{r_i}{\chi^2(r_i;0.025)}}\right)}_{\text{chi-square mid-interval estimate of the coefficient of variation}}\underbrace{\sqrt{\frac{1}{R_i}\sum_{k=1}^{R_i}\left(\frac{s_{ik}^{(condition)}}{\mu_{ik}^{(condition)}}\right)^2}}_{\text{pooled CV for all spots probing gene i}}\times 100\% \quad (2)$$

$\chi^2(r_i;\alpha)$ = chi-square for $r_i(=4R_i-1=$ number of degrees of freedom) and probability $\alpha$

$\mu_{ik}$ = average expression of gene i probed by spot k (= 1, ..., $R_i$) in the 4 biological replicas

$s_{ik}$ = standard deviation of the expression level of gene i probed by spot k

Preprints (www.preprints.org) | NOT PEER-REVIEWED | Posted: 15 June 2022 doi:10.20944/preprints202206.0214.v1

REV can be used to determine the Relative Expression Control (REC) of individual genes and the Pathway Relative Expression Control (PREC) of the (cardio) genomic fabric of a particular pathway:

$$REC_i^{(condition)} = \frac{\left\langle REV_i^{(condition)} \right\rangle\Big|_{\text{all genes}}}{REV_i^{(condition)}} - 1 \quad , \quad where:$$

$$\left\langle REV_i^{(condition)} \right\rangle\Big|_{\text{all genes}} = \text{median REV over the entire transcriptome} \tag{3}$$

$$PREC_{\Gamma}^{(condition)} = \frac{\left\langle REV_i^{(condition)} \right\rangle\Big|_{\text{all genes}}}{\left\langle REV_i^{(condition)} \right\rangle\Big|_{i\in\Gamma}} - 1 \tag{4}$$

$$where: \left\langle REV_i^{(condition)} \right\rangle\Big|_{\Gamma} = \text{median REV over the pathway } \Gamma$$

Higher positive REC values indicate genes whose random fluctuations of the expression level are strongly limited by the cellular homeostatic mechanisms within narrow intervals, most likely critical for the cell survival, phenotypic expression or/and integration in the multicellular structure of the myocardium. By contrast, lower negative RECs are associated with less controlled genes that can be vectors of cell adaptation to the slight fluctuations of the environmental conditions, as seen across biological replicas. Thus, REC indicates the non-uniform priorities of the cell in regulating the transcription machinery. Similarly, high positive PRECs are associated with critically important pathways to for the preservation of the phenotypic expression against environment changes and low PRECs with adapting pathways. One may observe that REC = 0 set the baseline for genes and PREC = 0 the baseline for the pathways. As presented in the Results section below, REC and PREC are sensitive to the external factors like ischemia and oxygen deprivation.

COR analysis is based on the Pearson product-moment correlation coefficient between the ($\log_2$) expressions of each gene *i* across biological replicas with each other gene *g* in the same group of replicas.

$$COR_{ig}^{(condition)} = \frac{\sum_{k_i=1}^{R_i}\sum_{k_g=1}^{Rg}\left(\sum_{j=1}^{4}\left(a_{i,k,j}^{(condition)} - AVE_i^{(condition)}\right)\left(a_{g,k,j}^{(condition)} - AVE_g^{(condition)}\right)\right)}{\sqrt{\sum_{k_i=1}^{R_i}\left(\sum_{j=1}^{4}\left(a_{i,k,j}^{(condition)} - AVE_i^{(condition)}\right)^2\right)\sum_{k_g=1}^{R_g}\left(\sum_{j=1}^{4}\left(a_{g,k,j}^{(condition)} - AVE_g^{(condition)}\right)^2\right)}} \tag{5}$$

Using COR analysis one can identify the ($p < 0.05$) significantly synergistically, antagonistically and independently expressed gene pairs. Two genes are synergistically expressed when their fluctuations across biological replicas go the same way and antagonistically expressed when their fluctuations go opposite ways. This analysis cannot determine which of the two genes is the master and which one is the slave. However, it says that when the master is up-regulated it forces the up-regulation of its synergistically expressed slaves and the down-regulation to the antagonistically expressed ones. Based on the "Principle of Transcriptomic Stoichiometry", COR determines the statistically significant parts of the gene networks in each condition separately, refining the gene "wiring" in functional pathways constructed by the dedicated software: Ingenuity Pathway Analysis [24], DAVID [25], KEGG [26] etc. Without COR analysis, the traditional pathways are the same regardless of race/strain, sex, age, heart region, and other factors known to influence the incidence of the disease, and the response to a treatment. Thus, GFP identifies for each patient in each condition the most stably expressed and interconnected gene network responsible for that particular biological process.

Moreover, GFP establishes the gene hierarchy in each condition using the Gene Commanding Height (GCH) scoring system that combines the expression control and expression coordination with each other gene.

Preprints (www.preprints.org) | NOT PEER-REVIEWED | Posted: 15 June 2022 doi:10.20944/preprints202206.0214.v1

$$GCH_i^{(condition)} = \left(REC_i^{(condition)} + 1\right) \times \exp\left( \underbrace{4\overline{COR_{ig}^2\Big|_{\forall g \neq i}^{(condition)}}}_{\text{average of squares}} - 1 \right) \tag{6}$$

The top of the hierarchy (highest GCH, termed Gene Master Regulator, GMR) is the gene whose strongly protected expression level is the most influential on the expression of other genes. By stably transfecting two human thyroid cancer cell lines with four genes, we proved that expression manipulation of a gene has transcriptomic consequences proportional to the GCH of that gene [27]. Because each cell phenotype has distinct gene hierarchy, smart manipulation of the GMR expression can be used to selectively kill, or by contrary, stimulate the proliferation of the desired cell type from a tissue.

*2.4. Comparing conditions of the (cardio) genomic fabric*

2.4.1. Cut-off criteria

When comparing two conditions (for instance "IN" with "NN" in the infarct experiment), traditional transcriptomic analysis uses uniform, arbitrary introduced cut-off for the absolute fold-change (1.5x or 2.0x) w/o requiring a less than 0.05 p-vale of the heteroscedastic *t*-test of the two means equality. However, such absolute fold-change cut-off might be too stringent for very stably expressed genes across biological replicas and low local technical noise while for other genes it might be too relaxed. Therefore, we determine the cut-off separately for each quantified gene so that the absolute fold-change criterion becomes:

$$\begin{gathered} \forall A = NN \vee N1 \vee N2 \vee N4; \quad \forall B = IN, IT \vee I1, C1 \vee I2, C2 \vee I4, C4 \\ \left|x_i^{(A\to B)}\right| > CUT_i^{(A\to B)} = 1 + \frac{1}{100}\sqrt{2\left(\left(REV_i^{(A)}\right)^2 + \left(REV_i^{(B)}\right)^2\right)} \quad , \quad where: \\ x_i^{(A\to B)} = \begin{cases} AVE_i^{(B)} / AVE_i^{(A)} & if \quad AVE_i^{(B)} \geq AVE_i^{(A)} \\ -AVE_i^{(A)} / AVE_i^{(B)} & if \quad AVE_i^{(B)} < AVE_i^{(A)} \end{cases} \end{gathered} \tag{7}$$

In addition to the absolute fold-change, our analysis maintains the p-value < 0.05 condition for the heteroscedastic t-test of the two means equality.

2.4.2. Uniform, weighted and all-inclusive contributions of individual genes to the transcriptome alteration

Traditional analysis measures the overall transcriptomic alteration by the percentages of the genes that were significantly up-/down-regulated or turned on/off. Such measure is limited to only the significantly regulated genes. Moreover, the regulated genes are considered as equal contributors to the transcriptome alteration, regardless of the how large is their departure from the normal expression level and what is the statistical confidence in their regulation.

A more informative measure is the **W**eighted **I**ndividual (gene) **R**egulation (WIR) [28] that takes into account the absolute departure from the normal expression level and the statistical confidence in the expression regulation:

$$WIR_i^{(A\to B)} = \underbrace{AVE_i^{(A)}\left(\left|x_i^{(A\to B)}\right| - 1\right)}_{\text{departure from the normal level}} \frac{x_i^{(A\to B)}}{\left|x_i^{(A\to B)}\right|} \underbrace{\left(1 - p_i^{(A\to B)}\right)}_{\text{confidence of regulation}} \tag{8}$$

$where: p_i^{(A\to B)}$ = p-val of the heteroscedastic t-test of $AVE_i^{(B)} = AVE_i^{(A)}$

Like the expression ratio "x", WIR takes also positive values for up-regulated genes and negative values for the down-regulated ones.

Preprints (www.preprints.org) | NOT PEER-REVIEWED | Posted: 15 June 2022 doi:10.20944/preprints202206.0214.v1

However, the best all-inclusive characterization of one gene contribution to the overall transcriptomic alteration is the "**I**ndividual (gene) **T**ranscriptomic **D**istance" (ITD). ITD is the magnitude of the 3D vector whose orthogonal components reflect the relative changes in the average expression level, expression variability (among biological replicas), and expression correlations (averaged over all other expressed genes) [29]:

$$ITD_i^{(A\to B)} \equiv \sqrt{\left(\frac{AVE_i^{(B)}-AVE_i^{(A)}}{\left\langle AVE_i^{(A)}\right\rangle_{all\ i}}\right)^2+\left(\frac{REV_i^{(B)}-REV_i^{(A)}}{\left\langle REV_i^{(A)}\right\rangle_{all\ i}}\right)^2+\frac{\left\langle\left(COR_{i,j}^{(B)}-COR_{i,j}^{(A)}\right)^2\right\rangle_{all\ j}}{\left\langle\left(COR_{i,j}^{(A)}\right)^2\right\rangle_{all\ j}}} \quad (9)$$

$$where: \left\langle Y_i^{(A)}\right\rangle_{\text{gene subset}} = \text{average characteristic "Y" over a gene subset in condition "A"}$$

Both WIR and ITD can be further averaged for a given functional pathway "Γ" as the Weighted Pathway Regulation (WPR) and **P**athway **T**ranscriptomic **T**rajectory (PTT), much more accurate in ranking the pathways according their alteration than the percentage of regulated genes:

$$WPR_\Gamma^{(A\to B)} = \frac{100}{\{\Gamma\}}\sqrt{\sum_{i\in\Gamma}\left(WIR_i^{(A\to B)}\right)^2} \quad , \quad \{\Gamma\} = \text{ number of genes in } \Gamma$$
$$PTD_\Gamma^{(A\to B)} = \frac{100}{\{\Gamma\}}\sqrt{\sum_{i\in\Gamma}\left(ITD_i^{(A\to B)}\right)^2} \quad (10)$$

*2.5. Transcriptomic effect of a treatment*

One can determine the transcriptomic effect of a treatment by comparing the alterations before and after that treatment. The comparison may encompass all genes or restricted to a particular functional pathway "Γ". Traditionally, such comparison is done by comparing the numbers of regulated genes with and without the treatment (when each gene is considered as a uniform contributor). In previous papers [13, 30, 31], we used the **G**ene **E**xpression **R**ecovery (GER). For instance, in the case of post-ischemic heart failure treated with bone marrow mononuclear cells (T), the genomic effects computed as GER takes into account not only the numbers of up- and down-regulated genes in IN whose normal expression was fully recovered in IT (i.e. {DX} and {UX}) but also the genes whose regulation status was not changed (i.e. {DD} and {UU}) and those whose regulation type was switched in IT (i.e. {DU} and (UD}).

$$GER_\Gamma^{(IN\to IT;NN)} = \frac{\underbrace{(\{DX\}+\{UX\})}_{\text{beneffic}} - \underbrace{(\{XD\}+\{XU\})}_{\text{side effects}}}{\underbrace{(\{DX\}+\{UX\})}_{\text{beneffic}} + \underbrace{(\{XD\}+\{UD\})}_{\text{side effects}} + \underbrace{(\{DD\}+\{UU\})}_{\text{residual alteration}} + \underbrace{(\{DU\}+\{UD\})}_{\text{overtreatment}}} \times 100\%$$

*where*: $D$ = "down", U = "up", X = "not"

$\{PQ\}$ = # of Γ-genes P =D/U/X regulated in IN and Q = D/U/X regulated in IT

Possible outcomes: (11)

1) $GER_\Gamma^{(IN\to IT;NN)} = 100\%$ (ideal) $\Leftarrow \{XD\}+\{XU\}=0 \ \wedge\ \{DD\}+\{UU\}=0 \ \wedge\ \{UD\}+\{DU\}=0$

2) $0<GER_\Gamma^{(IN\to IT;NN)}<100\%$ (positive) $\Leftarrow 0<\{XD\}+\{XU\}<\{DX\}+\{UX\}$

3) $GER_\Gamma^{(IN\to IT;NN)} = 0\%$ (null) $\Leftarrow \{DX\}+\{UX\}-\{XD\}-\{UD\}=0$

4) $GER_\Gamma^{(IN\to IT;NN)}<0$ (negative) $\Leftarrow \{XD\}+\{XU\}>\{DX\}+\{UX\}$

A better measure of the transcriptomic restoration compares the WPR scores, as the **P**athway **R**estoration **E**fficiency (PRE) [31]:

Preprints (www.preprints.org) | NOT PEER-REVIEWED | Posted: 15 June 2022 doi:10.20944/preprints202206.0214.v1

$$PRE_{\Gamma}^{(IN\to IT;NN)} = \left(1 - \frac{WPR_{\Gamma}^{(NN\to IT)}}{WPR_{\Gamma}^{(NN\to IN)}}\right) \times 100\% \quad (12)$$

Possible outcomes:

*a)* $WPR_{\Gamma}^{(NN\to IT)} = 0 \Rightarrow PRE_{\Gamma}^{(IN\to IT;NN)} = 100\%$ , *ideal*

*b)* $0 < WPR_{\Gamma}^{(NN\to IT)} < WPR_{\Gamma}^{(NN\to IN)} \Rightarrow 0 < PRE_{\Gamma}^{(IN\to IT;NN)} < 100\%$ , *positive*

*c)* $WPR_{\Gamma}^{(NN\to IT)} = WPR_{\Gamma}^{(NN\to IN)} \Rightarrow PRE_{\Gamma}^{(IN\to IT;NN)} = 0\%$ , *null*

*d)* $WPR_{\Gamma}^{(NN\to IT)} > WPR_{\Gamma}^{(NN\to IN)} \Rightarrow PRE_{\Gamma}^{(IN\to IT;NN)} < 0\%$ , *negative*

Now, we add the **C**omprehensive Pathway **R**estoration (CPR) representing the percent reduction of the Transcriptomic Distance in response to the treatment.

$$CPR_{\Gamma}^{(IN\to IT;NN)} = \left(1 - \frac{PTD_{\Gamma}^{(NN\to IT)}}{PTD_{\Gamma}^{(NN\to IN)}}\right) \times 100\% \quad (13)$$

Possible outcomes:

*a)* $PTD_{\Gamma}^{(NN\to IT)} = 0 \Rightarrow CPR_{\Gamma}^{(IN\to IT;NN)} = 100\%$ , *ideal*

*b)* $0 < PTD_{\Gamma}^{(NN\to IT)} < PTD_{\Gamma}^{(NN\to IN)} \Rightarrow 0 < CPR_{\Gamma}^{(IN\to IT;NN)} < 100\%$ , *positive*

*c)* $PTD_{\Gamma}^{(NN\to IT)} = PTD_{\Gamma}^{(NN\to IN)} \Rightarrow CPR_{\Gamma}^{(IN\to IT;NN)} = 0\%$ , *null*

*d)* $PTD_{\Gamma}^{(NN\to IT)} > PTD_{\Gamma}^{(NN\to IN)} \Rightarrow CPR_{\Gamma}^{(IN\to IT;NN)} < 0\%$ , *negative*

## 3. Results

### *3.1. Overview of the microarray data*

The PIHF experiment quantified the expression levels of 10,408 unigenes in all 12 samples from the groups "NN", "IN", "IT", n = 4/group), from which GFP extracted in each condition 10,408 AVEs + 10,408 REVs + 54,158,028 CORs = 54,178,844 values. Thus, GFP increased the size of the workable data in each condition by 5,206 times. With respect to NN, 579 genes (i.e. 5.56%) were significantly (according to our composite criterion) up-regulated and 1,222 (11.74%) were down-regulated in IN. The treatment with bone marrow mononuclear stem cells recovered partially the normal expression levels of the genes, leaving 256 (2.46%) up-regulated and 667 (6.41%) down-regulated in the IT group as compared with the NN controls. Interestingly, the treatment went even further by flipping the significant down-regulation of 19 genes and the significant up-regulation of 15 genes to their opposites.

In the hypoxia experiment, 9,716 unigenes were adequately quantified in all 36 samples from the groups "N1", "I1", "C1", "N2", "I2", "C2", "N4", "I4", "C4" (n = 4/group), from which GFP extracted in each condition 47,214,902 values. This is an increase by 4,860 times of the information used in the traditional analysis limited to the AVEs. According to our criterion, with respect to the control group "N1", 9.43% of the genes were up- and 11.72% were down-regulated in the group "I1", and 6.13% were up- and 4.30% down-regulated in "C1". With respect to "N2", 10.48% of the genes were up- and 18.94% were down-regulated in "I2", and 22.02% up- and 18.92% down-regulated in "C2". Finally, with respect to "N4", 4.08% were up- and 2.14% down in "I4", while in "C4", 6.01% were up- and 6.71% down-regulated.

### *3.2. AVE, REV and COR are independent features*

Figure 1 illustrates the evident independence of the AVE, REV and COR with Ank2 (ankyrin 2) for 34 genes involved in the inflammatory response in the left ventricle of the mice subjected for the first week of their life to normal atmospheric conditions ("N1"), or intermittent hypoxia ("I1") and constant hypoxia ("C1"). Supplementary Tables S1, S2, S3 presents the AVEs, REVs and CORs with Ank2 of the same genes for the 2 and 4 weeks of hypoxia exposures. The value 1 for the expression correlation of Ank2 with itself is the validation of the correctness of the COR analysis. Although Figure 1 is restricted to this

Preprints (www.preprints.org) | NOT PEER-REVIEWED | Posted: 15 June 2022 doi:10.20944/preprints202206.0214.v1

subset of genes, any other subset of genes in any other condition would prove the independence, including the ion channels and transporters in each of the four heart chambers of the adult mouse [6].

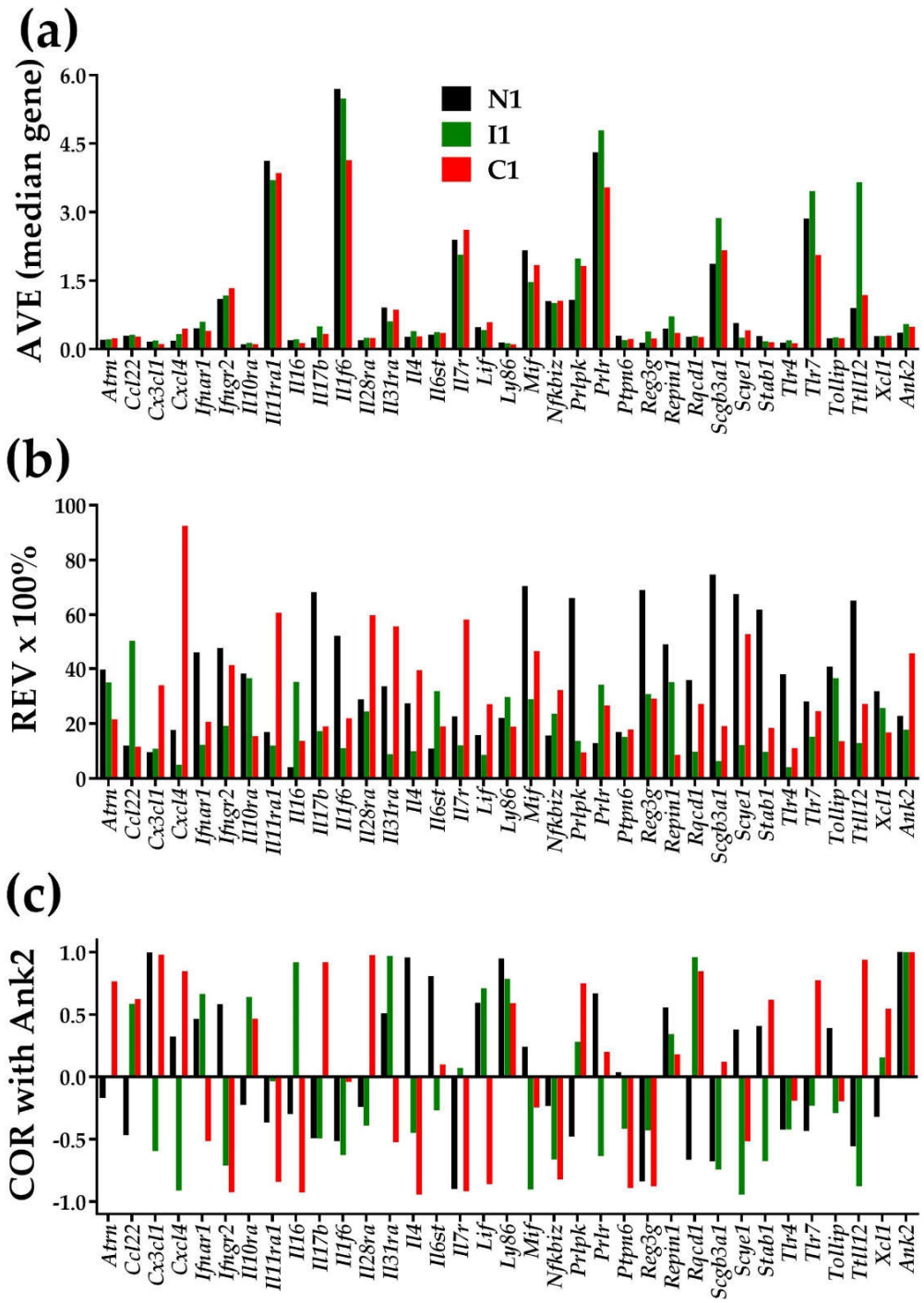


**Figure 1.** Illustration of the independence of the three types of characteristics of individual genes in the left ventricle of mice subjected in the first week of their life to normal atmospheric conditions ("N1"), chronic intermittent hypoxia ("I1"), or chronic constant hypoxia ("C1"). **(a)** Average expression level (AVE), in levels of the median gene in that condition. **(b)** Percentage of the Relative Expression Variability (REV); **(c)** Expression correlation with *Ank2*.

For reference, we added Table S1 presenting the genes with the largest expression level in each condition. For the 1-week exposure, the genes with the largest expression level were: Hspb6 (Heat shock protein, alpha-crystallin-related, B6; AVE = 14.19 in "N1"

Preprints (www.preprints.org) | NOT PEER-REVIEWED | Posted: 15 June 2022 doi:10.20944/preprints202206.0214.v1

and 9.64 in "C1") and Nr1i3 (Nuclear receptor subfamily 1, group I, member 3; AVE = 15.05 in "I1").

Likewise, in Table S2 we added the genes with the strongest expression control (i.e. lowest REV) in their respective treatment conditions. For the 1-week exposure, the most stably expressed genes were: Lias (Lipoic acid synthetase, REV = 1.4 in "N1"), Cadm4 (cell adhesion molecule 4, REV = 0.2 in "I1") and Numa1 (Nuclear mitotic apparatus protein 1, REV = 1.3 in "C1"). Of note is the diversity of the most controlled genes and how the left ventricle prioritized different genes in each of the distinct conditions.

Fig. 1 and Tables S1 – S3 also showed that chronic hypoxia not only changed the average expression level, but also the homeostatic control of the expression fluctuations and hence the expression variability across biological replicas. On top of this, hypoxia changed the expression coordination with other genes, illustrated here with *Ank2*, encoding Ankyrin-B one major player in cardiac physiology [32]). Coordination changes indicate remodeling of the gene networks. Through the analyses of expression variability and expression coordination, the GFP brings a treasure of previously neglected information about how the cardiac transcriptome is controlled and organized in partially overlapping networks.

### *3.3. Gene hierarchy*

GCH analysis was used to establish the hierarchies of the genes in the conditions "NN", "IN" and "IT". Figure 2 presents the top 20 genes in each condition. Of note is the lack of overlap among the three sets of top 20 genes, indicating distinct transcriptomic topologies. Remarkably, the top genes in one condition have low GCH scores in the other two. This finding can be used to selectively target the cells commanded by the GMRs in a mixture of cells like a tumor harboring cancer nodules within a mass of normal cells (e.g.: [21]). For these conditions, the GMRs are: Transmembrane protein 186 (Tmem186, with GCH = 53.21 in "NN", 1.03 in "IN" and 2.57 in "IT"), CD164 antigen (Cd164, with GCH = 1.54 in "NN", 46.37 in "IN" and 2.08 in "IT"), and ATPase type 13A2 (Atp13a2, with GCH = 1.88 in "NN", 0.99 in "IN" and 32.43 in "IT").

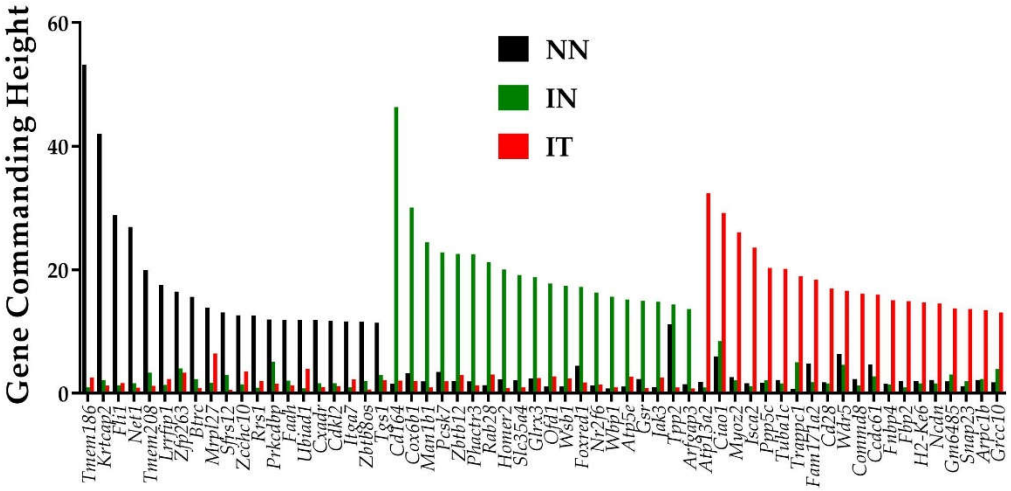


***Figure 2.*** Top 20 genes in the conditions: normal untreated ("NN"), infarcted untreated ("IN") and infarcted treated ("IT") normal untreated ("NN"), infarcted untreated ("IN") and infarcted treated ("IT"). Note there is no overlap of the three gene sets and that the top genes in one condition have low GCH scores in the other two conditions.

Some of the top hits in GCH analysis among the three conditions may represent some potentially new gene targets to protect heart against ischemic injury. For example, under IN condition, several genes that regulate cellular metabolism were among the top hits, suggesting adaptive responses to myocardial infarction. Most notably, the No. 2 gene hit

Preprints (www.preprints.org) | NOT PEER-REVIEWED | Posted: 15 June 2022 doi:10.20944/preprints202206.0214.v1

- Cox6b1 (cytochrome c oxidase, subunit 6B1) was shown to protect cardiomyocytes from hypoxia/reoxygenation injury by reducing ROS production and cell apoptosis [33]. The 4th gene hit - Pcsk7 (proprotein convertase subtilisin/kexin type 7) was also associated with cardiovascular disease phenotypes [34]. On the other hand, under IT condition, the 6th top hit gene - Tuba1c (tubulin, alpha 1C) was previously identified to predict the outcome of a linear combination of circadian rhythm pathway genes [35]. The 8th top gene was Fam171a2 (family with sequence similarity 171, member A2) and its transcript abundance in the heart was recently correlated with PR interval of electrocardiogram, suggesting a role for cardiac conduction system [36].

*3.4. Measures of expression regulation*

Figure 3 illustrates for 40 genes involved in the adrenergic signaling in cardiomyocyte [37] the four ways to report their transcriptomic alteration in infarcted untreated ("IN") and treated ("IT") heart with respect to normal condition.

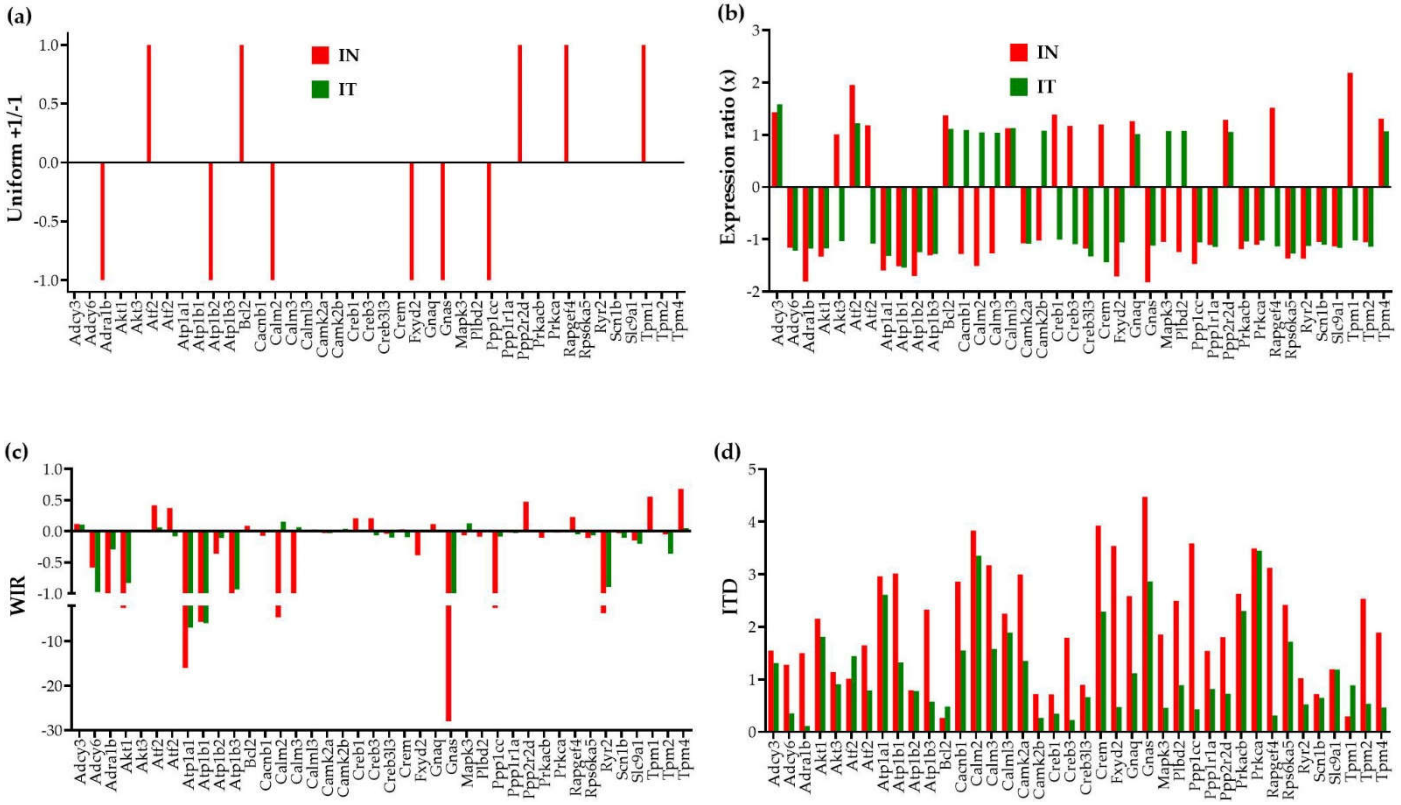


***Figure 3.*** Four ways to report the altered expression of 40 individual genes involved in the adrenergic signaling in cardiomyocytes in untreated ("IN") and treated ("IT") post ischemic infarcted mouse heart with respect to healthy counterparts. (a) Uniform +1/-1 contribution of significantly up-/down-regulated genes. (b) Expression ratios of all genes. (c) Weighted Individual (gene) Regulation (WIR). (d) Individual (gene) Transcriptomic Distance (ITD).

In the traditional analysis of the percentages of significantly up-/down-regulated genes, each affected gene is considered as a uniform +1 or -1 contributor to the overall transcriptomic regulation. Moreover, this measure is limited to the significantly regulated genes according to the criterion established by the investigator, frequently an arbitrary absolute fold-change cut-off. In our study, the absolute fold-change cut-off is determined separately for each expressed gene pending on its expression variability across biological replicas and the technical noise of the probing spot(s) in the microarray [14].

A better way to quantify the contributions of the individual genes to the overall transcriptomic alteration is to use the WIR score. Although still limited to the change in the

Preprints (www.preprints.org) | NOT PEER-REVIEWED | Posted: 15 June 2022 doi:10.20944/preprints202206.0214.v1

expression level, WIR not only considers all genes but weights their contribution according to the total absolute change of their expression level and the statistical confidence in their regulation. This measure was previously used to quantify the transcriptomic alterations in the left ventricle of a mouse model of Chagasic cardiomyopathy [28], in the cortical oligodendrocytes and microglia of a rabbit model of intra-ventricular hemorrhage [37], and in the hypothalamic arcuate node of a rat model of infantile spasms [31].

Nevertheless, the most comprehensive measure is the TD that takes into account the alterations of all independent characteristics of the individual genes. The new measures reveal that genes neglected because their expression ratios did not pass the threshold to be considered as significantly regulated may have even larger contributions to the transcriptome alteration than the significantly regulated ones. For instance, although the expression ratio of the significantly up-regulated Tpm1 (Tropomyosin 1, alpha) in "IN" (2.18x) is larger than that of the not significantly regulated Tpm4 (Tropomyosin 4, 1.31x), both WIR and ITD scores are larger for Tpm4 (WIR = 0.68, ITD = 1.89) than for Tpm1 (WIR = 0.55, ITD = 0.30) in "IN". Such findings imposes reconsideration of what really matters in the transcriptome changes. Interestingly, while Tpm1 is one of the main hypertrophic cardiomyopathy genes [38], Tpm4 is known for its inhibitory effect on actin polymerization [39].

Both "WIR" and "ITD" analyses revealed that for this pathway, the regulation of the Gnas gene, encoding the stimulatory alpha subunit, of the protein complex guanine nucleotide-binding protein (G protein), had the largest contribution to the transcriptomic alteration in "IN" (WIR = - 27.98, ITD = 4.47). Although, no longer significantly regulated in "IT" (x = - 1.12), Gnas still contributes to the transcriptomic differences with respect to the control "NN" (WIR = -1.67, ITD = 2.86). It was recently reported that a somatic mutation of Gnas is associated with focal, idiopathic right ventricular outflow tract (RVOT) tachycardia [40].

### *3.5. Regulation of the adrenergic signaling in the left ventricle of mice with post-ischemic heart failure*

Figure 4 presents the significant regulation of the genes involved in the adrenergic signaling in cardiomyocyte [41] as indicated by the microarray data in the left ventricle of mice with post-ischemic heart failure (condition "IN" with respect to "NN"). The pathway was designed by the Kanehisa Laboratories who developed the Kyoto Encyclopedia of Genes and Genomes (KEGG, [42]).

One may note that Adra1b (Adrenergic receptor, alpha 1b), involved in the positive regulation of the blood pressure [43], was significantly down-regulated (x = -1.81, WIR = -1.72, ITD = 1.50) in the infarcted heart. Although the other two subtypes of the alpha adrenergic receptors [44] were also down-regulated (Adra1a: x = -1.19, CUT = 1.65; Adra1d: x = -1.44, CUT = 1.73), their regulations were not statistically significant. However, because of larger differences in REVs and CORs, both genes had higher contributions to the overall alteration of the transcriptome than Adra1b, with ITD = 1.62 (Adra1a) and ITD = 1.67(Adra1d). It was reported that stimulation of these alpha adrenergic receptors can protect cardiomyocytes against ischemia by regulating the influx of glucose [45].

Preprints (www.preprints.org) | NOT PEER-REVIEWED | Posted: 15 June 2022 doi:10.20944/preprints202206.0214.v1

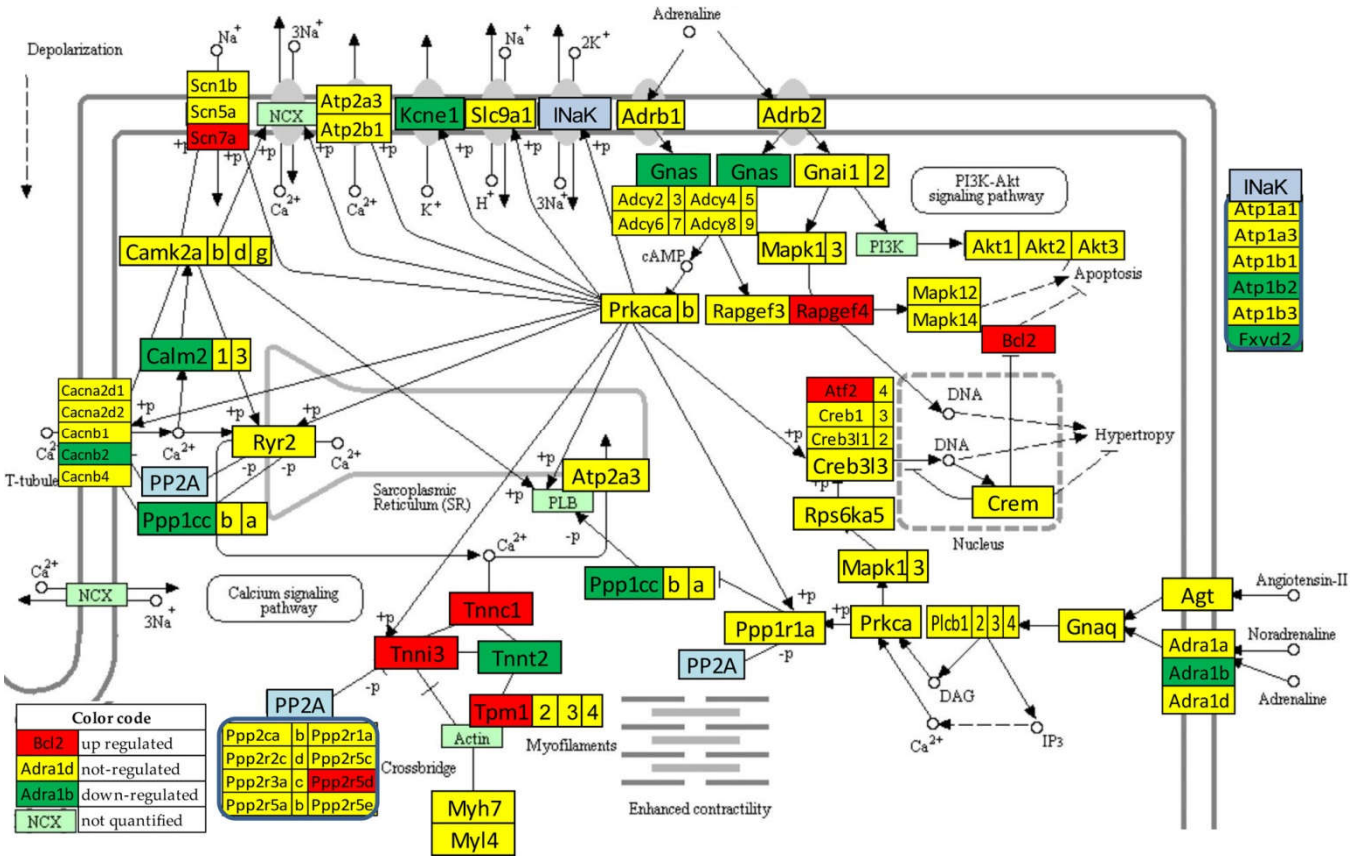


**Figure 4.** Statistically significant regulation of genes involved in the KEGG-built adrenergic signaling in the left ventricle cardiomyocytes of untreated mice with post-ischemic heart failure. INaK and PP2A are blocks of quantified genes, while NCX and PI3K are blocks of not quantified genes. Regulated genes: *Adra1b* (Adrenergic receptor, alpha 1b), *Atf2* (Activating transcription factor 2), *Atp1b2* (ATPase, Na+/K+ transporting, beta 2 polypeptide), *Bcl2* (B-cell leukemia/lymphoma 2), *Cacnb2* (Calcium channel, voltage-dependent, beta 2 subunit), *Calm2* (Calmodulin 2), *Fxyd2* (FXYD domain-containing ion transport regulator 2), *Gnas* (guanine nucleotide binding protein, alpha stimulating) complex locus), *Kcne1* (Potassium voltage-gated channel, Isk-related subfamily, member 1), *Ppp1cc* (Protein phosphatase 1, catalytic subunit, gamma isoform), *Ppp2r2d* (Protein phosphatase 2, regulatory subunit B, delta isoform), *Rapgef4* (Rap guanine nucleotide exchange factor (GEF) 4), *Scn7a* (Sodium channel, voltage-gated, type VII, alpha), and *Tpm1* (Tropomyosin 1, alpha).

### *3.6. Recovery of the adrenergic signaling in the left ventricle of mice with post-ischemic heart failure following treatment with bone marrow mononuclear stem cells*

Figure 5 presents the regulation of the adrenergic signaling in cardiomyocyte pathways after the stem cell treatment (condition "IT" with respect to "NN"). Of note is the recovery of the normal expression for: *Adra1b*, *Atp1b2*, *Bcl2*, *Cacnb2*, *Calm2*, *Fxyd2*, *Gnas*, *Ppp1cc*, *Ppp2r2d*, *Rapgef4*, *Scn7a*, and *Tpm1*. For this pathway, {DX} = 7, {UX} = 5, {XD} = 2, {XU} = 0, {DD} =1, {UU} = 0, {UD} = 0, {DU} = 0, so that $GER^{(IN \rightarrow IT;NN)} = 66.67\%$. $WPR^{(NN \rightarrow IN)} = 36.10$ and $WPR^{(NN \rightarrow IT)} = 13.63$, making $WPR^{(IN \rightarrow IT;NN)} = 62.24\%$. The transcriptomic distance analysis returned: $PTD^{(NN \rightarrow IN)} = 37.11$, $PTD^{(NN \rightarrow IT)} = 11.29$, resulting $CPR^{(IN \rightarrow IT;NN)} = 69.59\%$.

Preprints (www.preprints.org) | NOT PEER-REVIEWED | Posted: 15 June 2022 doi:10.20944/preprints202206.0214.v1

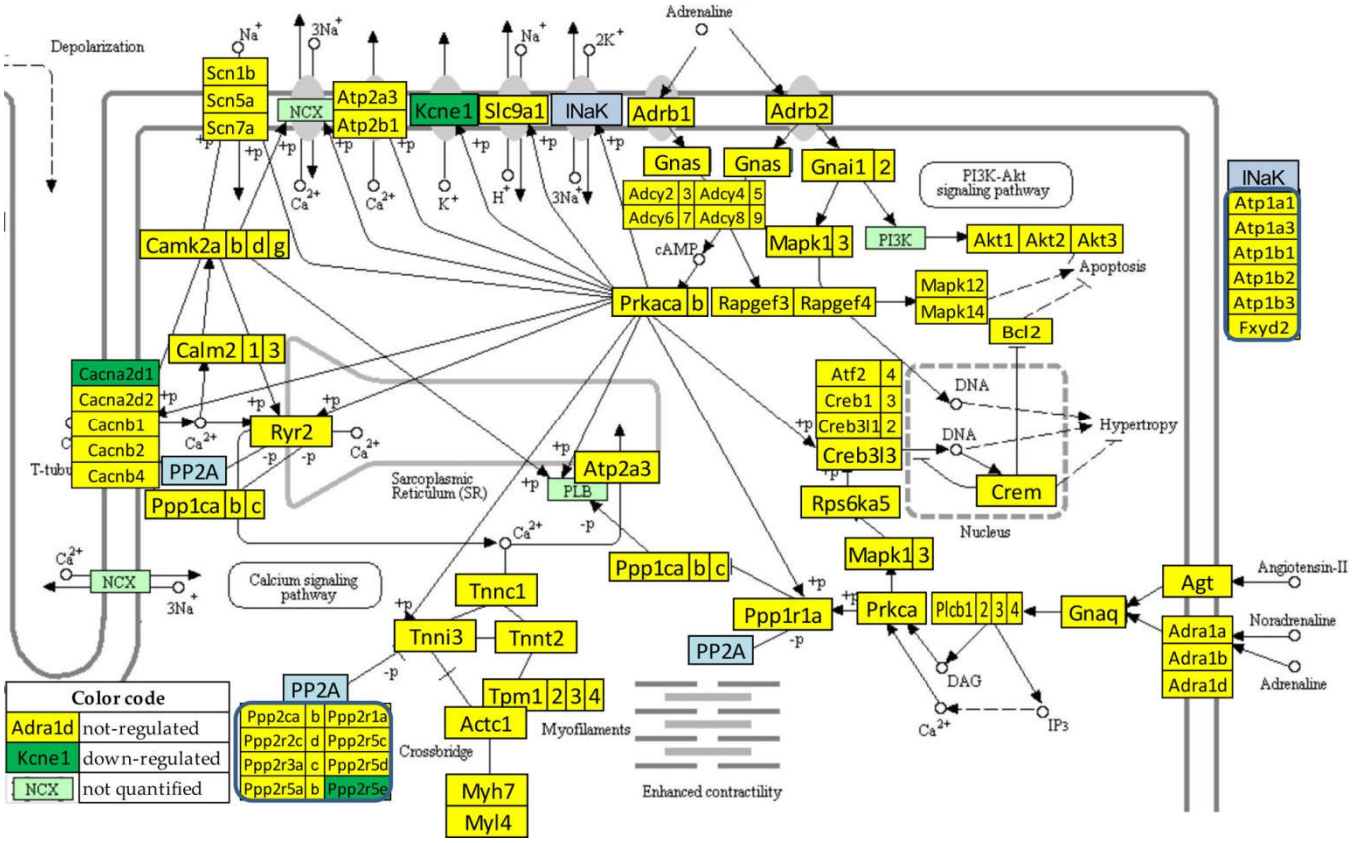


**Figure 5.** Statistically significant regulation of genes involved in the KEGG-built adrenergic signaling in the left ventricle cardiomyocytes of stem cell treated mice with post-ischemic heart failure. INaK and PP2A are blocks of quantified genes, while NCX and PI3K are blocks of not quantified genes. Regulated genes: *Cacna2d1* (Calcium channel, voltage-dependent, alpha2/delta subunit 1), *Kcne1* (Potassium voltage-gated channel, Isk-related subfamily, member 1), *Ppp2r5e* (Protein phosphatase 2, regulatory subunit B (B56), epsilon isoform).

### *3.7. Reconfiguration of the gene networks by the post-ischemic heart failure and recovery following treatment with bone marrow mononuclear stem cells*

Figure 6 illustrates the reconfiguration of the gene networks by the disease and following a treatment by showing how the infarct and the treatment affects the expression correlations of *Adra1b* with the other genes from the adrenergic signaling in cardiomyocytes. *Adra1b*, one of the six subtypes of the adrenergic receptors that control the heart contractility (inotropism) and rate (chronotropism), mediates its action by association with G proteins that activate a phosphatidylinositol-calcium second messenger system. In mouse, the alpha1-adrenergic receptors play adaptive roles in the heart and protect against the development of heart failure [46]. Figures 6abc present only the genes of the pathway that are statistically ($p < 0.05$) significant synergistically or antagonistically expressed with *Adra1b* in at least one of the three conditions. However, the percentages of the synergistically, antagonistically and independently expressed partners were computed for the entire pathway. Figure 6d lists the genes that are independently expressed with *Adra1b* in each condition.

Interestingly, as shown in panel (b), the infarct increased the synergistic partnership of *Adra1b* in this pathway from 13.9% to 24.1% and that of the antagonistic partnership from 1.3% to 8.9%. This very substantial strengthen of the *Adra1b* inter-coordination with many other genes of the pathway makes *Adra1b* a very important target to recover the altered heart functions. The treatment (panel (c)), reduced back the expression coordination to 11.4% synergism and 1.3% antagonism, and further decoupled numerous other genes from their correlation with *Adra1b* (panel (d): *Akt1*, *Atf2*, *Atf4*, *Atp1a3*, *Cacnb2*,

Preprints (www.preprints.org) | NOT PEER-REVIEWED | Posted: 15 June 2022 doi:10.20944/preprints202206.0214.v1

*Camk2a, Ppp2r2d, Ppp2r5d*). However, the treatment antagonistically coupled the independently expressed *Atf6b* and *Adra1b* under ischemic conditions.

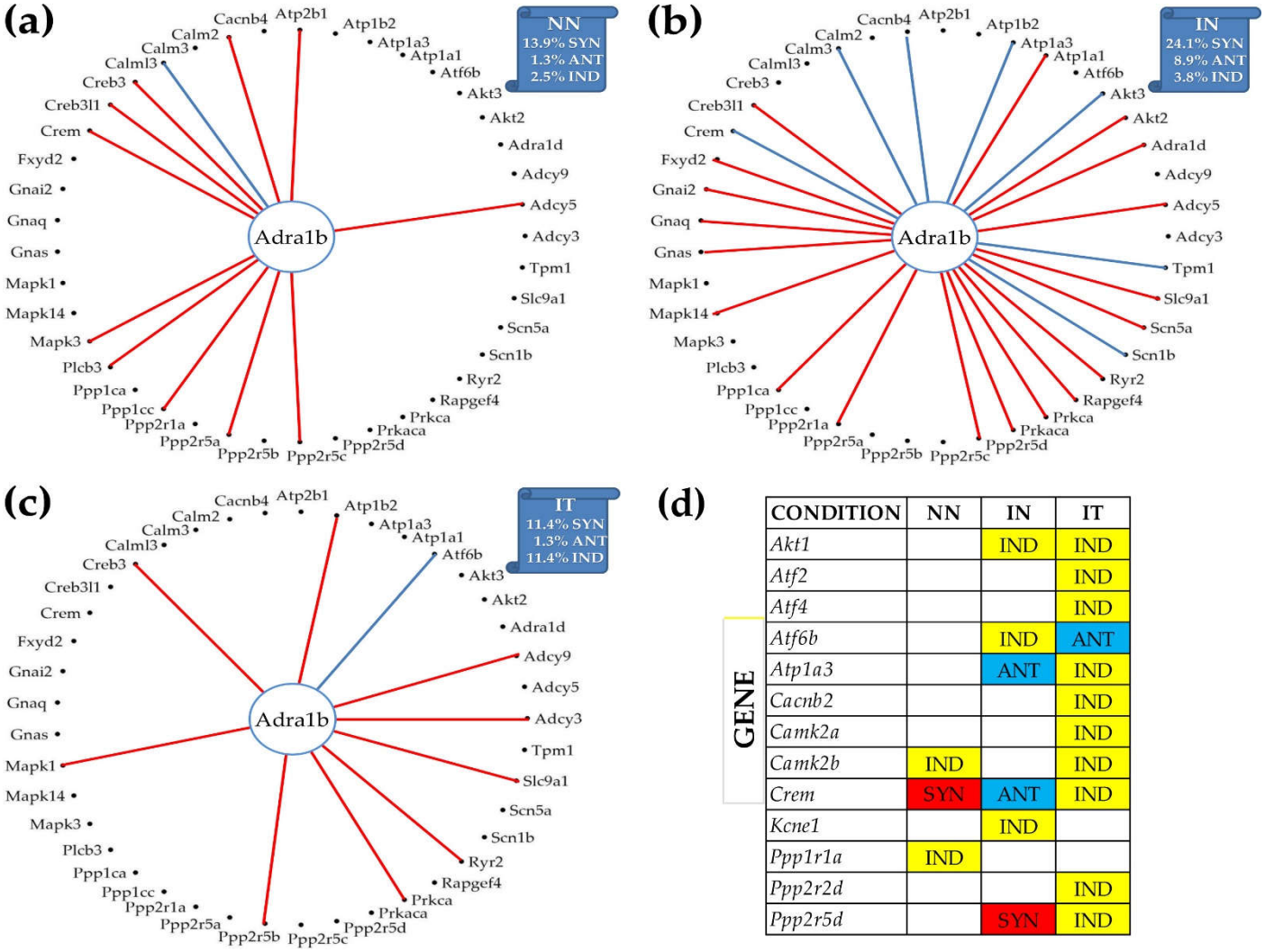


**Figure 6.** Remodeling of the *Adra1b* networking with genes from the functional pathway Adrenergic signaling in cardiomyocytes caused by the post ischemic heart failure with and without stem cell treatment. (a) Significantly synergistically and antagonistically expressed partners of *Adra1b* in "NN" hearts. (b) Significantly synergistically and antagonistically expressed partners of *Adra1b* in "IN" hearts. (c) Significantly synergistically and antagonistically expressed partners of *Adra1b* in "IT" hearts. (d) Independently expressed genes with *Adra1b.*

## 4. Discussion

The present study provides the theoretical bases of the (cardio)genomic fabric approach in identifying key gene regulatory factors. The theory is applied to expression data from the hearts of mouse models of common myocardial pathologies such as hypoxia and myocardial infarction with or without treatment with bone marrow mononuclear stem cells. Nevertheless, in a really personalized application, the biological replicas of diseased and normal cells should come from the same individual. Such procedure has been already used to compare samples collected from each cancer nodule and surrounding normal tissue from surgically removed tumors of thyroid [27, 47], kidney [29] and prostate [48, 49]. For cardiac diseases, one can collect samples from localized heart myocardium using percutaneus endomyocardial biopsy [50].

Through considering three independent groups of characteristics for each individual gene in each condition (illustrated in Fig. 1), GFP run through the full potential of profiling tens of thousands of transcripts at a time on several biological replicas. The independence

 doi:10.20944/preprints202206.0214.v1

and complementarity of the 3 types of characteristics was proved previously for genes within mTOR signaling pathway and evading apoptosis in human prostate [45, 46], apoptosis in human thyroid [27] and chemokine signaling in human kidney [29]. They were also proved for chemokine signaling in mouse cortex [48], PI3K–AKT signaling in mouse hippocampus [49], and ion channels and transporters in mouse heart myocardia of each of the four chambers [6]. Regardless of the used RNA-sequencing or microarrayplatform, this strategy increased by 4-5 orders of magnitude the workable information furnished by a high throughput transcriptomic study.

As one may note in Fig.1, the hypoxia not only changed the expression levels of the individual genes, but also their expression control and expression coordination in fucntional pathways. Substantial changes in the genes' expression control and inter-coordination were constant findings in all previous GFP studies on diseases on samples collected from both humans [29, 47-49] and animal models (e.g.: [31, 51-54]). We believe that such rich additional information could be instrumental in developing a personalized genomic medicine.

GFP provides essential clues on the priorities of the cellular homeostatic mechanisms in controlling the expression of critical genes and especially how the genes are networked to optimize the functional pathways. That Lias is the most protected gene in the heart of 1 week normoxic mice did not come as surprise given the strong antioxidant potency of the $\alpha$-lipoidic acid synthesized by the encoded enzyme [55]. Lias was significantly upregulated (x = 1.52) in ischemic heart but its expression was restored to normal by the cell treatment. Cadm4, the most protected gene in the heart of mice subjected during their first week of life to chronic intermittent hypoxia, is essential for restricting the production of cardiac outflow tract progenitor cells in zebrafish [56]. Whether it performs a similar function for the development of the mouse heart remains to be tested by further experiments. Finaly, Numa1, the most protected gene after 1 week chronic constant hypoxia is a marker of the myotonic dystrophy type 1 [57].

Importantly, GFP can hierarchize the genes according to their Gene Commanding Height (GCH, Fig. 2) that accounts for both the strength of the homeostatic controlling mechanisms of the expression accuracy and power to regulate expression of other genes. With GCH, one can identify the gene master regulator of that condition (GMR) whose "smart" manipulation would have the desired effect on the cells it commands but little to no consequences on the other cells of the tissue. The monotonic relationship between the GCH and the transcriptomic consequences of altering the expression of that gene was proved by stable transfection of 4 genes into two standard human thyroid cancer cell lines [47, 58].

Nonetheless, our approach improves quantification of the transcriptome alteration with a more accurate absolute fold-change cut-off to decide about the statistical significance of the expression regulation (Eq. 7) and especially with more comprehanssive measures of individual gene contributions (Eqs. 8, 9). Fig. 3 makes a powerful case of the importance of addopting WIR and ITD for a better understanding of the transcriptomic consequences of a disease.

One of our primary focuses was on the key genes regulating myocardial adrenergic signaling, such as Adra1b, (Figures 4 to 6), by means of the KEGG-built platform. The cardioprotective role of Adra1b has long been established by Woodcock's group who first showed the reduction of reperfusion-induced Ins(1,4,5)P3 generation and arrhythmias in mouse hearts expressing constitutively active alpha1B-adrenergic receptors [59]. However, under pathologic conditions, e.g. pressure overload, overexpressing of alpha1B-adrenergic receptors leads to depressed contractile responses to beta- adrenergic receptor activation, and predispose hearts to hypertrophy and worsen heart failure [60].

Our present study further revealed the remodeling of the Adra1b networking following myocardial infarction (group IN) and normalization by the post myocardial infarction stem cell treatment (group IT) (Figure 6). The coordination analysis provided additional insights that would not be available through simple comparison of expression levels of

individual genes. For instance, Crem (CAMP responsive element modulator) coordination with Adra1b was switched from synergistic in "NN" to antagonistic in "IN", and practically independent in "IT", indicating major change in the interaction of the two genes. While the critical role of Crem in β-adrenoreceptor-mediated cardiac dysfunction is documented [61], there is not yet any report concerning the interaction between Crem and Adra1b and how such interection might impact the heart physiology. Since Crem is a transcription factor that mediates high glucose response in cardiomyocytes [62], its relationship with Adra1b deserves further investigation.

## 5. Conclusions

So far, the GFP power to represent the organization of the transcriptome was successfully tested in several other studies on neurological diseases (e.g.: [31, 51-53]), pulmonary hypertension [54] and cancers [27, 29, 47-49]. GFP proved also its ability to characterize the transcriptomic networks linking ionic channels and transporters across the heart chambers [6] as well as different cell types in insert systems [63]. The present report provides evidence of the advantages of using GFP analyses to decode the remodeling of the gene networks in the myocardialtissue following myocardial infraction or systemic hypoxia.

**Supplementary Materials: Table S1**: Average expression (AVE) normalized to the median gene expression levels of 34 inflammatory response genes, *Ank2* and the genes with the largest expression level in the entire transcriptome after 2 and 4 weeks exposure to normal atmospheric conditions (N2, N4), chronic intermittent hypoxia (I1, I2) and chronic constant hypoxia (C2, C4); **Table S2**: Relative expression variation (REV) of 34 inflammatory response genes, *Ank2* and the most stably expressed genes in the entire transcriptome after 2 and 4 weeks exposure to normal atmospheric conditions (N2, N4), chronic intermittent hypoxia (I1, I2) and chronic constant hypoxia (C2, C4); **Table S3**: Expression correlation with *Ank2* of 34 genes after 2 and 4 weeks exposure to normal atmospheric conditions (N2, N4), chronic intermittent hypoxia (I1, I2) and chronic constant hypoxia (C2, C4).

**Author Contributions:** Conceptualization, D.A.I. and L.X.; methodology, D.A.I.; software, D.A.I.; validation, D.A.I. and L.X.; formal analysis, D.A.I.; investigation, D.A.I.; resources, D.A.I. and L.X.; data curation, D.A.I. and L.X.; writing—original draft preparation, D.A.I. and L.X.; writing—review and editing, D.A.I. and L.X.; visualization, D.A.I.; supervision, D.A.I.; project administration, D.A.I. Both authors have read and agreed to the published version of the manuscript.

**Funding:** This research received no external funding.

**Data Availability Statement:** Experimental data used in this report were collected from the publicly accessible Gene Expression Omnibus (GEO) data bases: https://www.ncbi.nlm.nih.gov/sites/GDSbrowser?acc=GDS3655, https://www.ncbi.nlm.nih.gov/geo/query/acc.cgi?acc=GSE29769 https://www.ncbi.nlm.nih.gov/geo/query/acc.cgi?acc=GSE2271

**Conflicts of Interest:** The authors declare no conflict of interest.

## References

1. Kanuri, S.H.; Ipe, J.; Kassab, K.; Gao, H.; Liu, Y.; Skaar, T.C.; Kreutz, R.P. Next generation MicroRNA sequencing to identify coronary artery disease patients at risk of recurrent myocardial infarction. *Atherosclerosis* **2018,** *278*:232-239. doi: 10.1016/j.atherosclerosis.2018.09.021
2. Khera, A.V.; Kathiresan, S. Genetics of coronary artery disease: discovery, biology and clinical translation. *Nat Rev Genet* **2017,** *18*:331-344. doi: 10.1038/nrg.2016.160
3. Friede, K.A.; Myers, R.A.; Gales, J.; Zhbannikov, I.; Ortel, T.L.; Shah, S.H.; Kraus, W.E.; Ginsburg, G.S.; Voora, D. An antiplatelet response gene expression signature is associated with bleeding. *Cardiovasc Res*. **2022** :cvac079. doi: 10.1093/cvr/cvac079.
4. Nath, M.; Romaine, S.P.; Koekemoer, A.; Hamby, S.; Webb, T.R.; Nelson, C.P.; Castellanos-Uribe, M.; Papakonstantinou, M.; Anker, S.D.; Lang, C.C. et al. Whole blood transcriptomic profiling identifies molecular pathways related to cardiovascular mortality in heart failure. *Eur J Heart Fail*. **2022**. doi: 10.1002/ejhf.2540. Online ahead of print.
5. He, X.; Liu, J.; Gu, F.; Chen, J.; Lu, Y.W.; Ding, J.; Guo, H.; Nie, M.; Kataoka, M.; Lin, Z.; et al. Cardiac CIP protein regulates dystrophic cardiomyopathy. *Mol Ther*. **2022**; 30(2):898-914. doi: 10.1016/j.ymthe.2021.08.022.

6. Iacobas, S.; Amuzescu, B.; Iacobas, D.A. Transcriptomic uniqueness and commonality of the ion channels and transporters in the four heart chambers, *Sci Rep* **2021,** *11*(1):2743. https://doi.org/10.1038/s41598-021-82383-1.
7. Iacobas, D.A.; Iacobas, S.; Lee, P.R.; Cohen, J.E.; Fields, R.D. Coordinated Activity of Transcriptional Networks Responding to the Pattern of Action Potential Firing in Neurons. *Genes (Basel)* **2019**, *10*(10), 754. Doi: 10.3390/genes10100754.
8. Iacobas, S.; Iacobas, D.A.; Spray, D.C.; Scemes, E. The connexin43 transcriptome during brain development: importance of genetic background. *Brain Research* **2012**; *1487*: 131-139. doi: 10.1016/j.brainres.2012.05.062.
9. Thomas, N.M.; Jasmin, J.F.; Lisanti, M.P.; Iacobas, D.A. Sex Differences in Expression and subcellular Localization of Heart Rhythm Determinant Proteins. *Biochem Biophys Res Commun* **2011;** *406*(1):117-22. doi: 10.1016/j.bbrc.2011.02.006.
10. Iacobas, D.A.; Fan, C.; Iacobas, S.; Spray, D.C.; Haddad, G.G. Transcriptomic changes in developing kidney exposed to chronic hypoxia. *Biochem Biophys Res Comm* **2006;**. 349(1), 329-338. DOI:10.1016/j.bbrc.2006.08.056.
11. Lachtermacher, S.; Esporcatte, B.L.B.; Montalvo, F.; Costa, P.C.; Rodrigues, D.C.; Belem, L.; Rabischoffsky, A.; Neto, H.F.; Vasconcellos, R.; Iacobas, D.A. *et al*. Cardiac gene expression and systemic cytokine profile are complementary in a murine model of post ischemic heart failure. *Braz J Med Biol Res*. **2010,** *43*(4):377-89. DOI: 10.1590/s0100-879x2010007500014.
12. Transcriptomic effects of law salt diet on the mouse left ventricle. Available on line: https://www.ncbi.nlm.nih.gov/geo/query/acc.cgi?acc=GSE72561. Accessed: 12/05/2021
13. Lachtermacher, S.; Esporcatte, B.L.B.; Fortes, F.S.A.; Rocha, L.L.; Montalvo, F.; Costa, P.; Belem, L.; Rabischoffsky, A.; Neto, H.F.; Vasconcellos, R.; Iacobas, D.A.; *et al*. Functional and Transcriptomic Recovery of Infarcted Mouse Myocardium Treated with Bone Marrow Mononuclear Cells. *Stem Cell Rev*. **2011,** *8*(1):251-61. doi: 10.1007/s12015-011-9282-2.
14. Lee, P.R.; Cohen, J.E.; Iacobas, D.A.; Iacobas, S.; Fields, R.D. Gene networks activated by pattern-specific generation of action potentials in dorsal root ganglia neurons. *Sci Rep*. **2017**, *7*:43765, doi:10.1038/srep43765.
15. Fan, C.; Iacobas, D.A.; Zhou, D.; Chen, Q.; Gavrialov, O.; Haddad, G.G. Gene expression and phenotypic characterization of mouse heart after chronic constant and intermittent hypoxia. *Physiol Genomics* **2005,** *22*: 292-307. DOI: 10.1152/physiolgenomics.00217.2004.
16. Goldenberg, R.C.S.; Iacobas, D.A.; Iacobas, S.; Rocha, L.L.; Fortes, F.S.A.; Vairoa, L.; Nagajyothi, F.; deCarvalho, A.C.C.; Tanowitz, H.B.; Spray, D.C. Transcriptomic alterations in *Trypanosoma cruzi*-infected cardiac myocytes. *Microbes Infect* **2009,** *11*(14-15):1140-9. doi:10.1016/j.micinf.2009.08.009.
17. Adesse, D.; Iacobas, D.A.; Iacobas, S.; Garzoni, L.R.; Meirelles Mde N.; Tanowitz, H.B.; Spray, D.C. Transcriptomic signatures of alterations in a myoblast cell line infected with four strains of *Trypanosoma cruzi*. *Am J Trop Med Hyg*. **2010**, *82*(5): 846-54. doi: 10.4269/ajtmh.2010.09-0399.
18. Post-ischemic heart failure model. Available on line: https://www.ncbi.nlm.nih.gov/sites/GDSbrowser?acc=GDS3655. Accessed 12/1/2021.
19. Functional and Transcriptomic Recovery of Infarcted Mouse Myocardium Treated with Bone Marrow Mononuclear Cells. Available on line: https://www.ncbi.nlm.nih.gov/geo/query/acc.cgi?acc=GSE29769. Accessed 12/1/2021.
20. Gene expression and phenotypic characterization of mouse heart after chronic constant or intermittent hypoxia. Available on line: https://www.ncbi.nlm.nih.gov/geo/query/acc.cgi?acc=GSE2271. Accessed 12/1/2021.
21. Iacobas, D.A.; Fan, C.; Iacobas, S.; Haddad, G.G. Integrated transcriptomic response to cardiac chronic hypoxia: translation regulators and response to stress in cell survival. *Funct Integr Genomics* **2008**. *8*(3):265-75. doi: 10.1007/s10142-008-0082-y.
22. Iacobas, D.A.; Iacobas, S.; Haddad, G.G. Heart rhythm genomic fabric in hypoxia. *Biochem Biophys Res Commun* **2010**. *391*(4):1769-1774. doi: 10.1016/j.bbrc.2009.12.151.
23. Iacobas, S.; Iacobas, D.A. Effects of Chronic Intermittent Hypoxia on Cardiac Rhythm Transcriptomic Networks. In: *Intermittent Hypoxia and Human Diseases*, Xi, L. & Serebrovskaya, T.V. (Editors): New York: Springer, U.S.A., 2012. Pp. 15-28.
24. https://digitalinsights.qiagen.com/products-overview/discovery-insights-portfolio/analysis-and-visualization/qiagen-ipa/
25. https://david.ncifcrf.gov
26. https://www.kegg.jp/kegg/pathway.html
27. Iacobas, D.A. Biomarkers, Master Regulators and Genomic Fabric Remodeling in a Case of Papillary Thyroid Carcinoma. *Genes (Basel)* **2020**. *11*(9):E1030. https://doi.org/10.3390/genes11091030.
28. Iacobas, D.A.; Iacobas, S.; Tanowitz, H.B.; deCarvalho, A.C.; Spray, D.C. Functional genomic fabrics are remodeled in a mouse model of Chagasic cardiomyopathy and restored following cell therapy. *Microbes Infect*. **2018,** 20(3), 185-195. doi: 10.1016/j.micinf.2017.11.003.
29. Iacobas, D.A.; Mgbemena, V.E.; Iacobas, S.; Menezes, K.M.; Wang, H.; Saganti, P.B. Genomic Fabric Remodeling in Metastatic Clear Cell Renal Cell Carcinoma (ccRCC): A New Paradigm and Proposal for a Personalized Gene Therapy Approach. *Cancers* **2020,** *12*(12) 3678. PMID: 33302383, DOI: 10.3390/cancers12123678.
30. Soares, M.B.; Lima, R.S.; Souza, B.S.F.; Vasconcelos, J.F.; Rocha, L.L, dos Santos, R.R.; Iacobas, S.; Goldenberg, R.C.; Iacobas, D.A.; Tanowitz, H.B.; Spray, D.C.; Campos de Carvalho, A.C. Reversion of gene expression alterations in hearts of mice with chronic chagasic cardiomyopathy after transplantation of bone marrow cells. *Cell cycle* **2011**, *10*(9): 1448-1455. doi: 10.4161/cc.10.9.15487. PMCID:PMC3117044.
31. Iacobas, D.A.; Chachua, T.; Iacobas, S.; Benson, M.J.; Borges, K.; Veliskova, J.; Velisek, L. ACTH and PMX53 recover the normal synaptic transcriptome in a rat model of infantile spasms. *Sci Rep* **2018** 8:5722, DOI:10.1038/s41598-018-24013-x.
32. Koenig, S.N.; Mohler, P.J. The evolving role of ankyrin-B in cardiovascular disease. *Heart Rhythm* **2017,** *14*(12):1884-1889. https://doi.org/10.1016/j.hrthm.2017.07.032.

33. Zhang, W.; Wang, Y.; Wan, J.; Zhang, P.; Pei, F. COX6B1 relieves hypoxia/reoxygenation injury of neonatal rat cardiomyocytes by regulating mitochondrial function. *Biotechnol Lett*. **2019,** *41*(1):59-68. doi: 10.1007/s10529-018-2614-4.
34. Yao, C.; Chen, B.H.; Joehanes, R.; Otlu, B.; Zhang, X.; Liu, C.; Huan, T.; Tastan,; O.; Cupples, L.A.; Meigs, J.B. et al. Integromic analysis of genetic variation and gene expression identifies networks for cardiovascular disease phenotypes. *Circulation*. **2015**; *131*(6):536-49. doi: 10.1161/CIRCULATIONAHA.114.010696. Erratum in: *Circulation*. **2015**; *131*(19):e474.
35. Yan, X.; Huang, Y.; Wu, J. Identify Cross Talk Between Circadian Rhythm and Coronary Heart Disease by Multiple Correlation Analysis. *J Comput Biol*. **2018**; *25*(12):1312-1327. doi: 10.1089/cmb.2017.0254.
36. Adriaens, M.E.; Lodder E.M.; Moreno-Moral, A.; Šilhavý, J.; Heinig, M.; Glinge, C.; Belterman C.; Wolswinkel, R.; Petretto, E.; Pravenec, M. et al. Systems Genetics Approaches in Rat Identify Novel Genes and Gene Networks Associated With Cardiac Conduction. *J Am Heart Assoc*. 2018; *7*(21):e009243. doi: 10.1161/JAHA.118.009243.
37. Krishna, S.; Cheng, B.; Sharma, D.R.; Yadav, S.; Stempinski, E.; Mamtani, S.; Shah, E.; Deo, A.; Acherjee, T.; Thomas, T. et al. PPARG activation enhances myelination and neurological recovery in premature rabbits with intraventricular hemorrhage. *PNAS* **2021**. *118* (36) e2103084118. https://doi.org/10.1073/pnas.2103084118.
38. Lamounier Junior A, Guitián González A, Rodríguez Vilela A, Repáraz Andrade A, Rubio Alcaide Á, Berta Sousa A, Benito López C, Alonso García D, Fernández Ferro G. et al. Genotype-phenotype correlations in hypertrophic cardiomyopathy: a multicenter study in Portugal and Spain of the TPM1 p.Arg21Leu variant. *Rev Esp Cardiol* (Engl Ed). **2022**; 75(3):242-250. doi: 10.1016/j.rec.2021.01.001.
39. Wu, N.; Xu, J.; Du, W.W.; Li, X.; Awan, F. M.; Li, F.; Misir, S.; Eshaghi, E.; Lyu, J.; Zhou, L. et al. YAP Circular RNA, circYap, Attenuates Cardiac Fibrosis via Binding with Tropomyosin-4 and Gamma-Actin Decreasing Actin Polymerization. *Mol Ther* **2021**, *29*(3), 1138–1150. https://doi.org/10.1016/j.ymthe.2020.12.004
40. Ip JE, Xu L, Dai J, Steegborn C, Jaffré F, Evans T, Cheung JW, Basson CT, Panaghie G, Krogh-Madsen T, Abbott GW, Lerman BB. Constitutively Activating GNAS Somatic Mutation in Right Ventricular Outflow Tract Tachycardia. Circ Arrhythm Electrophysiol. 2021 Oct;14(10):e010082. doi: 10.1161/CIRCEP.121.010082.
41. Adrenergic signaling in cardiomyocytes. Available on line: https://www.genome.jp/kegg-bin/show_pathway?mmu04261, accessed 12/07/2021
42. Kanehisa, M.; Furumichi, M.; Tanabe, M.; Sato, Y.; Morishima, K. KEGG: new perspectives on genomes, pathways, diseases and drugs. *Nucleic Acids Res*. **2017,** *45*, D353–D361. DOI: 10.1093/nar/gkw1092.
43. Cotecchia, S.; Björklöf, K.; Rossier, O.; Stanasila, L.; Greasley, P.; Fanelli, F. The alpha1b-adrenergic receptor subtype: molecular properties and physiological implications. *J Recept Signal Transduct Res*. **2002**; 22(1-4):1-16. doi: 10.1081/rrs-120014585.
44. Perez, D.M.; Doze, V.A. Cardiac and neuroprotection regulated by $\alpha$(1)-adrenergic receptor subtypes. *J Recept Signal Transduct Res*. **2011**; 31(2):98-110. doi: 10.3109/10799893.2010.550008.
45. Shi, T.; Papay, R.S.; Perez, D.M. $\alpha$1A-Adrenergic receptor prevents cardiac ischemic damage through PKCδ/GLUT1/4-mediated glucose uptake. *J Recept Signal Transduct Res*. **2016**;b36(3):261-70. doi: 10.3109/10799893.2015.1091475.
46. Jensen, B.C.; Swigart, P.M.; De Marco, T.; Hoopes, C.; Simpson, P.C. {alpha}1-Adrenergic receptor subtypes in nonfailing and failing human myocardium. *Circulation. Heart failure* **2009**, *2*(6), 654–663. https://doi.org/10.1161/CIRCHEARTFAILURE.108.846212.
47. Iacobas, D.A.; Tuli, N.; Iacobas, S.; Rasamny, J.K.; Moscatello, A.; Geliebter, J.; Tiwari, R.M. Gene master regulators of papillary and anaplastic thyroid cancer phenotypes. *Oncotarget* **2018,** 9(2), 2410-2424. doi: 10.18632/oncotarget.23417.
48. Iacobas, S.; Iacobas, D.A. A Personalized Genomics Approach of the Prostate Cancer. *Cells* **2021**, 10, 1644. https://www.mdpi.com/2073-4409/10/7/1644
49. Iacobas, S.; Iacobas, D.A. Personalized 3-Gene Panel for Prostate Cancer Target Therapy. *Curr. Issues Mol. Biol.* **2022**, *44*, 360-382. https://doi.org/10.3390/cimb44010027
50. Xu, Xiqi; Tian, Zhuang; Fang, Quan; Jing, Zhi-Cheng; Zhang, Shuyang∗ Standard Operation Procedure of Percutaneous Endomyocardial Biopsy in Peking Union Medical College Hospital, Cardiology Discovery: September 2021 - Volume 1 - Issue 3 - p 148-153 doi: 10.1097/CD9.0000000000000023.
51. Iacobas, D.; Wen, J.; Iacobas, S.; Schwartz, N.; Putterman, C. Remodeling of Neurotransmission, Chemokine, and PI3K-AKT Signaling Genomic Fabrics in Neuropsychiatric Systemic Lupus Erythematosus. *Genes* **2021**, *12*, 251. https://doi.org/10.3390/genes12020251
52. Iacobas, D.A.; Wen, J.; Iacobas, S.; Putterman, C.; Schwartz, N. TWEAKing the Hippocampus: The Effects of TWEAK on the Genomic Fabric of the Hippocampus in a Neuropsychiatric Lupus Mouse Model. *Genes* **2021**, 12(8), 1172; https://doi.org/10.3390/genes12081172.
53. Victorino, P.H.; Marra, C.; Iacobas, D.A.; Iacobas, S.; Spray, D.C.; Linden, R.; Adesse, D.; Petrs-Silva, H. Retinal Genomic Fabric Remodeling after Optic Nerve Injury. Genes 2021, 12, 403. https://doi.org/10.3390/genes12030403
54. Mathew, R.; Huang, J.; Iacobas, S.; Iacobas, D.A. Pulmonary Hypertension Remodels the Genomic Fabrics of Major Functional Pathways. *Genes* **2020**, *11*, 126. https://doi.org/10.3390/genes11020126
55. Tian, S.; Nakamura, J.; Hiller, S.; Simington, S.; Holley, D.W.; Mota, R.; Willis, M.S.; Bultman, S.J.; Luft, J.C.; DeSimone, J.M.; et al. New insights into immunomodulation via overexpressing lipoic acid synthase as a therapeutic potential to reduce atherosclerosis. *Vascul Pharmacol*. **2020**; 133-134:106777. doi: 10.1016/j.vph.2020.106777.
56. Zeng, X.X.; Yelon, D. Cadm4 restricts the production of cardiac outflow tract progenitor cells. *Cell Rep*. **2014**; *7*(4):951-60. doi: 10.1016/j.celrep.2014.04.013.

57. Dastidar, S.; Majumdar, D.; Tipanee, J.; Singh, K.; Klein, A.F.; Furling, D.; Chuah, M.K.; VandenDriessche, T. Comprehensive transcriptome-wide analysis of spliceopathy correction of myotonic dystrophy using CRISPR-Cas9 in iPSCs-derived cardiomyocytes. *Mol Ther*. **2022**; *30*(1):75-91. doi: 10.1016/j.ymthe.2021.08.004.
58. Iacobas, S.; Ede, N.; Iacobas, D.A. The Gene Master Regulators (GMR) Approach Provides Legitimate Targets for Personalized, Time-Sensitive Cancer Gene Therapy. *Genes* **2019**, *10*, 560. https://doi.org/10.3390/genes10080560
59. Harrison, S.N.; Autelitano, D.J.; Wang, B.H.; Milano, C.; Du, X.J.; Woodcock, E.A. Reduced reperfusion-induced Ins(1,4,5)P3 generation and arrhythmias in hearts expressing constitutively active alpha1B-adrenergic receptors. *Circ Res*. **1998**; *83*(12):1232-40. doi: 10.1161/01.res.83.12.1232.
60. Woodcock, E.A. Roles of alpha1A- and alpha1B-adrenoceptors in heart: insights from studies of genetically modified mice. *Clin Exp Pharmacol Physiol*. **2007**; *34*(9):884-8. doi: 10.1111/j.1440-1681.2007.04707.x.
61. Lewin, G.; Matus, M.; Basu, A.; Frebel, K.; Rohsbach, S.P.; Safronenko, A.; Seidl, M.D.; Stümpel, F.; Buchwalow, I.; König, S. et al. Critical role of transcription factor cyclic AMP response element modulator in beta1-adrenoceptor-mediated cardiac dysfunction. *Circulation*. **2009**; 119(1):79-88. doi: 10.1161/CIRCULATIONAHA.108.786533.
62. Barbati, S.A.; Colussi, C.; Bacci, L.; Aiello, A.; Re, A.; Stigliano, E,.;Isidori, A.M.; Grassi, C.; Pontecorvi, A.; Farsetti, A. et al Transcription Factor CREM Mediates High Glucose Response in Cardiomyocytes and in a Male Mouse Model of Prolonged Hyperglycemia. *Endocrinology*. **2017**; *158*(7):2391-2405. doi: 10.1210/en.2016-1960.
63. Iacobas, D.A.; Iacobas, S.; Stout, R.F.; Spray, D.C. Cellular Environment Remodels the Genomic Fabrics of Functional Pathways in Astrocytes. *Genes* **2020**, *11*, 520. https://doi.org/10.3390/genes11050520

Preprints (www.preprints.org) | NOT PEER-REVIEWED | Posted: 15 June 2022 doi:10.20944/preprints202206.0214.v1

| Symbol | Gene | N2 | I2 | C2 | N4 | I4 | C4 |
|---|---|---|---|---|---|---|---|
| Atrn | Attractin | 0.27 | 0.30 | 0.24 | 0.31 | 0.21 | 0.36 |
| Ccl22 | Chemokine (C-C motif) ligand 22 | 0.29 | 0.29 | 0.27 | 0.28 | 0.25 | 0.26 |
| Cx3cl1 | Chemokine (C-X3-C motif) ligand 1 | 0.16 | 0.15 | 0.29 | 0.21 | 0.24 | 0.23 |
| Cxcl4 | Chemokine (C-X-C motif) ligand 4 | 0.27 | 0.12 | 0.41 | 0.23 | 0.33 | 0.28 |
| Ifnar1 | Interferon (alpha and beta) receptor 1 | 0.27 | 0.20 | 0.58 | 0.24 | 0.29 | 0.27 |
| Ifngr2 | Interferon gamma receptor 2 | 1.23 | 1.07 | 1.21 | 1.05 | 0.94 | 0.76 |
| Il10ra | Interleukin 10 receptor, alpha | 0.18 | 0.14 | 0.15 | 0.11 | 0.13 | 0.08 |
| Il11ra1 | Interleukin 11 receptor, alpha chain 1 | 3.47 | 4.94 | 4.48 | 6.86 | 5.94 | 5.52 |
| Il16 | Interleukin 16 | 0.20 | 0.17 | 0.27 | 0.14 | 0.12 | 0.21 |
| Il17b | Interleukin 17B | 0.50 | 0.38 | 0.10 | 0.49 | 0.42 | 0.29 |
| Il1f6 | Interleukin 1 family, member 6 | 5.44 | 4.18 | 5.42 | 7.21 | 7.19 | 6.80 |
| Il28ra | Interleukin 28 receptor alpha | 0.29 | 0.16 | 0.18 | 0.25 | 0.16 | 0.15 |
| Il31ra | Interleukin 31 receptor A | 0.88 | 0.47 | 1.78 | 0.89 | 0.85 | 1.32 |
| Il4 | Interleukin 4 | 0.71 | 0.49 | 0.30 | 0.26 | 0.27 | 0.25 |
| Il6st | Interleukin 6 signal transducer | 0.36 | 0.42 | 0.34 | 0.32 | 0.41 | 0.51 |
| Il7r | Interleukin 7 receptor | 2.14 | 3.01 | 1.75 | 3.04 | 3.27 | 2.85 |
| Lif | Leukemia inhibitory factor | 0.49 | 0.48 | 0.61 | 0.35 | 0.45 | 0.33 |
| Ly86 | Lymphocyte antigen 86 | 0.21 | 0.19 | 0.11 | 0.16 | 0.16 | 0.15 |
| Mif | Macrophage migration inhibitory factor | 0.85 | 1.35 | 2.00 | 0.82 | 0.62 | 0.73 |
| Nfkbiz | Nuclear factor of kappa light polypeptide gene enhancer in B-cells inhibitor, zeta | 1.14 | 1.29 | 0.85 | 1.45 | 1.66 | 1.20 |
| Prlpk | Prolactin-like protein K | 2.06 | 1.83 | 0.88 | 2.78 | 3.31 | 2.45 |
| Prlr | Prolactin receptor | 10.23 | 11.07 | 5.99 | 7.25 | 7.12 | 4.05 |
| Ptpn6 | Protein tyrosine phosphatase, non-receptor type 6 | 0.32 | 0.13 | 0.48 | 0.26 | 0.20 | 0.36 |
| Reg3g | Regenerating islet-derived 3 gamma | 0.34 | 0.33 | 0.13 | 0.40 | 0.43 | 0.16 |
| Repin1 | Replication initiator 1 | 0.96 | 0.29 | 0.70 | 0.55 | 0.59 | 0.51 |
| Rqcd1 | Rcd1 (required for cell differentiation) homolog 1 (S. pombe) | 0.22 | 0.15 | 0.30 | 0.23 | 0.19 | 0.33 |
| Scgb3a1 | Secretoglobin, family 3A, member 1 | 1.90 | 1.50 | 1.36 | 4.03 | 2.55 | 4.77 |
| Scye1 | Small inducible cytokine subfamily E, member 1 | 0.24 | 0.38 | 0.43 | 0.18 | 0.15 | 0.09 |
| Stab1 | Stabilin 1 | 0.26 | 0.33 | 0.21 | 0.20 | 0.20 | 0.10 |
| Tlr4 | Toll-like receptor 4 | 0.14 | 0.18 | 0.25 | 0.18 | 0.19 | 0.08 |
| Tlr7 | Toll-like receptor 7 | 3.02 | 2.71 | 4.08 | 4.82 | 3.49 | 4.61 |
| Tollip | Toll interacting protein | 0.24 | 0.19 | 0.34 | 0.17 | 0.21 | 0.15 |
| Ttll12 | Tubulin tyrosine ligase-like family, member 12 | 2.96 | 4.69 | 3.88 | 4.57 | 3.37 | 4.05 |
| Xcl1 | Chemokine (C motif) ligand 1 | 0.30 | 0.26 | 0.23 | 0.33 | 0.29 | 0.40 |
| Ank2 | Ankyrin 2, brain | 0.26 | 0.20 | 0.32 | 0.22 | 0.36 | 0.34 |
| *Hspb6* | *Heat shock protein, alpha-crystallin-related, B6* | *14.52* | ***16.51*** | ***14.12*** | *23.04* | *14.11* | *20.58* |
| *Nr1i3* | *Nuclear receptor subfamily 1, group I, member 3* | ***19.61*** | *11.60* | *5.42* | ***24.96*** | ***18.97*** | ***21.06*** |

**Table S1: Average expression (AVE) normalized to the median gene expression levels of 34 inflammatory response genes, *Ank2* and the genes with the largest expression level in the entire transcriptome after 2 and 4 weeks exposure to normal atmospheric conditions (N2, N4), chronic intermittent hypoxia (I1, I2) and chronic constant hypoxia (C2, C4).** Light gray background indicates the genes with the largest expression level within the selection while the darker gray indicates the gene with the largest expression level in each condition.

Preprints (www.preprints.org) | NOT PEER-REVIEWED | Posted: 15 June 2022 doi:10.20944/preprints202206.0214.v1

| Symbol | Gene | N2 | I2 | C2 | N4 | I4 | C4 |
|---|---|---|---|---|---|---|---|
| Atrn | Attractin | 5.6 | 20.9 | 13.9 | 43.1 | 12.9 | 42.3 |
| Ccl22 | Chemokine (C-C motif) ligand 22 | 13.0 | 15.2 | 31.0 | 5.2 | 23.0 | 27.2 |
| Cx3cl1 | Chemokine (C-X3-C motif) ligand 1 | 29.9 | 28.7 | 13.8 | 30.8 | 20.0 | 14.5 |
| Cxcl4 | Chemokine (C-X-C motif) ligand 4 | 30.6 | 19.5 | 14.2 | 33.5 | 31.9 | 36.6 |
| Ifnar1 | Interferon (alpha and beta) receptor 1 | 14.7 | 45.6 | 16.3 | 58.7 | 20.2 | 16.0 |
| Ifngr2 | Interferon gamma receptor 2 | 14.1 | 29.3 | 16.0 | 40.0 | 18.2 | 36.8 |
| Il10ra | Interleukin 10 receptor, alpha | 21.9 | ***66.2*** | 27.6 | 34.8 | 21.4 | 47.3 |
| Il11ra1 | Interleukin 11 receptor, alpha chain 1 | 18.2 | 46.2 | 19.5 | 49.5 | 10.3 | 28.0 |
| Il16 | Interleukin 16 | 13.1 | 9.1 | 8.7 | 16.9 | 22.8 | ***54.0*** |
| Il17b | Interleukin 17B | 15.3 | 30.3 | 35.5 | 12.0 | 13.6 | 24.2 |
| Il1f6 | Interleukin 1 family, member 6 | 16.9 | 22.9 | 38.5 | 26.1 | 15.5 | 34.0 |
| Il28ra | Interleukin 28 receptor alpha | 22.6 | 15.5 | 36.1 | 10.7 | 33.8 | 32.0 |
| Il31ra | Interleukin 31 receptor A | 33.2 | 62.3 | 22.1 | 3.2 | 22.7 | 34.1 |
| Il4 | Interleukin 4 | ***48.5*** | 15.3 | ***47.4*** | 22.1 | 18.7 | 39.4 |
| Il6st | Interleukin 6 signal transducer | 8.8 | 32.8 | 19.8 | 14.6 | 27.0 | 33.8 |
| Il7r | Interleukin 7 receptor | 12.2 | 68.2 | 31.2 | 75.7 | 18.1 | 28.4 |
| Lif | Leukemia inhibitory factor | 4.0 | 4.8 | 20.5 | 13.3 | 14.9 | 19.1 |
| Ly86 | Lymphocyte antigen 86 | 15.7 | 30.1 | 29.6 | 32.2 | 19.0 | 50.0 |
| Mif | Macrophage migration inhibitory factor | 7.4 | 39.4 | 14.1 | 51.2 | 41.6 | 41.9 |
| Nfkbiz | Nuclear factor of kappa light polypeptide gene enhancer in B-cells inhibitor, zeta | 10.4 | 12.3 | 18.9 | 12.4 | 16.3 | 36.5 |
| Prlpk | Prolactin-like protein K | 7.9 | 21.9 | 16.2 | 35.4 | 32.7 | 25.3 |
| Prlr | Prolactin receptor | 15.8 | 12.1 | 6.3 | 29.9 | ***51.8*** | 52.7 |
| Ptpn6 | Protein tyrosine phosphatase, non-receptor type 6 | 38.0 | 40.0 | 25.3 | 27.8 | 34.6 | 35.8 |
| Reg3g | Regenerating islet-derived 3 gamma | 19.6 | 38.5 | 46.0 | 38.4 | 42.7 | 10.6 |
| Repin1 | Replication initiator 1 | 27.8 | 29.6 | 24.0 | 7.7 | 38.8 | 37.8 |
| Rqcd1 | Rcd1 (required for cell differentiation) homolog 1 (S. pombe) | 22.0 | 23.4 | 30.4 | 24.4 | 19.9 | 42.0 |
| Scgb3a1 | Secretoglobin, family 3A, member 1 | 35.3 | 22.8 | 16.6 | 10.5 | 45.3 | 8.9 |
| Scye1 | Small inducible cytokine subfamily E, member 1 | 5.6 | 44.1 | 30.8 | ***64.7*** | 36.7 | 41.0 |
| Stab1 | Stabilin 1 | 26.3 | 20.1 | 9.5 | 29.2 | 18.8 | 39.6 |
| Tlr4 | Toll-like receptor 4 | 20.1 | 32.3 | 14.6 | 40.5 | 27.2 | 8.0 |
| Tlr7 | Toll-like receptor 7 | 10.5 | 18.7 | 22.3 | 16.9 | 11.8 | 5.0 |
| Tollip | Toll interacting protein | 8.9 | 45.5 | 24.6 | 56.9 | 15.3 | 22.4 |
| Ttll12 | Tubulin tyrosine ligase-like family, member 12 | 15.0 | 25.5 | 32.3 | 30.8 | 8.9 | 46.2 |
| Xcl1 | Chemokine (C motif) ligand 1 | 15.2 | 10.6 | 3.4 | 17.1 | 18.8 | 16.3 |
| Ank2 | Ankyrin 2, brain | 31.5 | 52.0 | 17.7 | ***64.6*** | 23.3 | 21.8 |
| *Ankrd15* | *Ankyrin repeat domain 15* | *0.5* | *53.3* | *18.9* | *47.0* | *6.2* | *16.0* |
| *Tubg1* | *Tubulin, gamma 1* | *4.7* | *0.4* | *10.7* | *19.4* | *62.5* | *19.1* |
| *Dmkn* | *Dermokine* | *16.3* | *11.6* | *1.1* | *11.9* | *14.3* | *57.3* |
| *Mrpl15* | *Mitochondrial ribosomal protein L15* | *12.0* | *11.8* | *14.5* | *1.3* | *15.3* | *16.8* |
| *Qtrtd1* | *Queuine tRNA-ribosyltransferase domain containing 1* | *11.9* | *14.2* | *9.7* | *25.2* | *1.3* | *32.1* |
| *Arid2* | *AT rich interactive domain 2 (Arid-rfx like)* | *20.6* | *37.4* | *8.9* | *37.9* | *12.0* | *0.6* |

**Table S2: Relative expression variation (REV) of 34 inflammatory response genes, *Ank2* and the most stably expressed genes in the entire transcriptome after 2 and 4 weeks exposure to normal atmospheric conditions (N2, N4), chronic intermittent hypoxia (I1, I2) and chronic constant hypoxia (C2, C4).** Light gray background indicates the genes with the largest expression control (i.e. lowest REV) level within the selection while the darker gray indicates the gene with the largest control in the entire condition. Bold Italics indicate the largest variabilities in the selected gene subset.

Preprints (www.preprints.org) | NOT PEER-REVIEWED | Posted: 15 June 2022 doi:10.20944/preprints202206.0214.v1

| Symbol | Gene | N2 | I2 | C2 | N4 | I4 | C4 |
|---|---|---|---|---|---|---|---|
| Atrn | Attractin | -0.567 | 0.409 | -0.944 | 0.674 | 0.839 | 0.160 |
| Ccl22 | Chemokine (C-C motif) ligand 22 | -0.677 | 0.837 | -0.349 | 0.001 | -0.483 | 0.620 |
| Cx3cl1 | Chemokine (C-X3-C motif) ligand 1 | 0.937 | 0.900 | 0.355 | 0.962 | 0.793 | -0.541 |
| Cxcl4 | Chemokine (C-X-C motif) ligand 4 | 0.981 | -0.416 | -0.025 | 0.909 | -0.227 | 0.783 |
| Ifnar1 | Interferon (alpha and beta) receptor 1 | 0.768 | 0.920 | 0.897 | 0.991 | 0.776 | 0.844 |
| Ifngr2 | Interferon gamma receptor 2 | 0.929 | 0.932 | 0.725 | 0.950 | 0.295 | 0.959 |
| Il10ra | Interleukin 10 receptor, alpha | -0.412 | -0.828 | -0.616 | 0.529 | -0.418 | -0.482 |
| Il11ra1 | Interleukin 11 receptor, alpha chain 1 | 0.951 | -0.979 | -0.885 | -0.998 | 0.212 | -0.809 |
| Il16 | Interleukin 16 | -0.920 | 0.300 | 0.508 | 0.484 | 0.531 | 0.809 |
| Il17b | Interleukin 17B | 0.581 | -0.964 | 0.092 | 0.144 | -0.472 | -0.190 |
| Il1f6 | Interleukin 1 family, member 6 | -0.990 | 0.779 | -0.211 | -0.993 | -0.598 | 0.010 |
| Il28ra | Interleukin 28 receptor alpha | 0.920 | -0.866 | -0.074 | 0.802 | -0.119 | -0.646 |
| Il31ra | Interleukin 31 receptor A | 0.989 | 0.972 | 0.765 | 0.501 | 0.635 | 0.679 |
| Il4 | Interleukin 4 | -0.910 | 0.265 | 0.092 | 0.009 | 0.753 | -0.037 |
| Il6st | Interleukin 6 signal transducer | 0.858 | 0.903 | 0.994 | 0.681 | 0.574 | -0.762 |
| Il7r | Interleukin 7 receptor | -0.925 | -0.975 | -0.910 | -0.969 | -0.598 | -0.047 |
| Lif | Leukemia inhibitory factor | 0.764 | 0.701 | 0.179 | -0.649 | 0.761 | 0.118 |
| Ly86 | Lymphocyte antigen 86 | -0.996 | -0.972 | -0.117 | 0.814 | 0.609 | 0.402 |
| Mif | Macrophage migration inhibitory factor | -0.369 | -0.885 | 0.682 | 0.873 | -0.544 | 0.470 |
| Nfkbiz | Nuclear factor of kappa light polypeptide gene enhancer in B-cells inhibitor, zeta | -0.891 | -0.832 | -0.413 | -0.730 | -0.042 | -0.946 |
| Prlpk | Prolactin-like protein K | -0.313 | -0.780 | -0.955 | 0.707 | 0.059 | -0.781 |
| Prlr | Prolactin receptor | -0.988 | 0.543 | -0.550 | 0.370 | -0.127 | -0.990 |
| Ptpn6 | Protein tyrosine phosphatase, non-receptor type 6 | -0.940 | -0.679 | -0.519 | 0.530 | -0.323 | 0.111 |
| Reg3g | Regenerating islet-derived 3 gamma | 0.923 | -0.943 | -0.017 | -0.975 | -0.239 | -0.296 |
| Repin1 | Replication initiator 1 | -0.942 | 0.683 | -0.856 | 0.676 | -0.357 | 0.688 |
| Rqcd1 | Rcd1 (required for cell differentiation) homolog 1 (S. pombe) | 0.820 | 0.828 | -0.217 | 0.814 | 0.034 | 0.687 |
| Scgb3a1 | Secretoglobin, family 3A, member 1 | -0.944 | -0.774 | -0.951 | -0.471 | -0.108 | -0.287 |
| Scye1 | Small inducible cytokine subfamily E, member 1 | 0.213 | 0.684 | 0.776 | 0.920 | -0.580 | -0.052 |
| Stab1 | Stabilin 1 | -0.724 | -0.639 | 0.341 | 0.913 | -0.860 | -0.229 |
| Tlr4 | Toll-like receptor 4 | 0.789 | 0.948 | -0.831 | -0.980 | -0.172 | -0.595 |
| Tlr7 | Toll-like receptor 7 | -0.927 | 0.607 | -0.476 | 0.022 | -0.446 | 0.304 |
| Tollip | Toll interacting protein | -0.026 | 0.997 | 0.931 | 0.983 | 0.950 | 0.980 |
| Ttll12 | Tubulin tyrosine ligase-like family, member 12 | -0.887 | -0.919 | -0.183 | 0.524 | -0.183 | -0.638 |
| Xcl1 | Chemokine (C motif) ligand 1 | 0.757 | -0.852 | -0.825 | 0.184 | 0.342 | 0.252 |
| Ank2 | Ankyrin 2, brain | | | | | | |

**Table S3: Expression coordination of 34 inflammatory response genes with *Ank2* after 2 and 4 weeks exposure to normal atmospheric conditions (N2, N4), chronic intermittent hypoxia (I1, I2) and chronic constant hypoxia (C2, C4).** Red/blue/yellow background indicates statistically ($p < 0.05$) significant synergistic/antagonistic/independent expression of that gene with *Ank2*, while black background indicates perfect positive correlation (COR =1) of *Ank2* with itself.